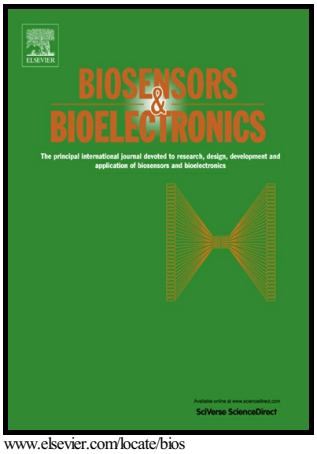

www.elsevier.com/locate/bios

Current Advances and Future Visions on Bioelectronic Immunosensing for Prostate-specific Antigen

Conlathan Ibau, M.K. Md Arshad, Subash C.B. Gopinath

PII: S0956-5663(17)30434-7
DOI: http://dx.doi.org/10.1016/j.bios.2017.06.049
Reference: BIOS9819

To appear in: *Biosensors and Bioelectronic*

Received date: 3 April 2017
Revised date: 13 June 2017
Accepted date: 25 June 2017

Cite this article as: Conlathan Ibau, M.K. Md Arshad and Subash C.B. Gopinath Current Advances and Future Visions on Bioelectronic Immunosensing fo Prostate-specific Antigen, *Biosensors and Bioelectronic* http://dx.doi.org/10.1016/j.bios.2017.06.049

Current Advances and Future Visions on Bioelectronic Immunosensing for Prostate-specific Antigen

Conlathan Ibau[a], M.K. Md Arshad[a,b*], Subash C.B. Gopinath[a,c]

[a]Institute of Nano Electronic Engineering (INEE), Universiti Malaysia Perlis (UniMAP), 01000 Kangar, Perlis, Malaysia

[b]School of Microelectronic Engineering (SoME), Universiti Malaysia Perlis (UniMAP), Pauh Putra Campus, 02600 Arau, Perlis, Malaysia

[c]School of Bioprocess Engineering, Universiti Malaysia Perlis (UniMAP), 02600 Arau, Perlis, Malaysia

[*]Correspondence to: Institute of Nano Electronic Engineering (INEE), Universiti Malaysia Perlis (UniMAP), Perlis, Malaysia. Tel.: +604 9798581; fax: +604 9798578. mohd.khairuddin@unimap.edu.my

Abstract

Early cancer diagnosis remains the holy-grail in the battle against cancers progression. Tainted with debates and medical challenges, current therapeutic approaches for prostate cancer (PCa) lack early preventive measures, rapid diagnostic capabilities, risk factors identification, and portability, i.e. the inherent attributes offered by the label-free biosensing devices. Electronic assisted immunosensing systems inherit the high sensitivity and specificity properties due to the predilection of the antigen–antibody affinity. Bioelectronic immunosensor for PCa has attracted much attentions among the researchers due to its high-performance, easy to prepare, rapid feedback, and possibility for miniaturization. This review explores the current advances on bioelectronic immunosensors for the detection of PCa biomarker revealed in the past decade. The research milestones and current trends of the immunosensors are reported to project the future visions in order to propel their "lab-to-market" realization.

Graphical Abstract

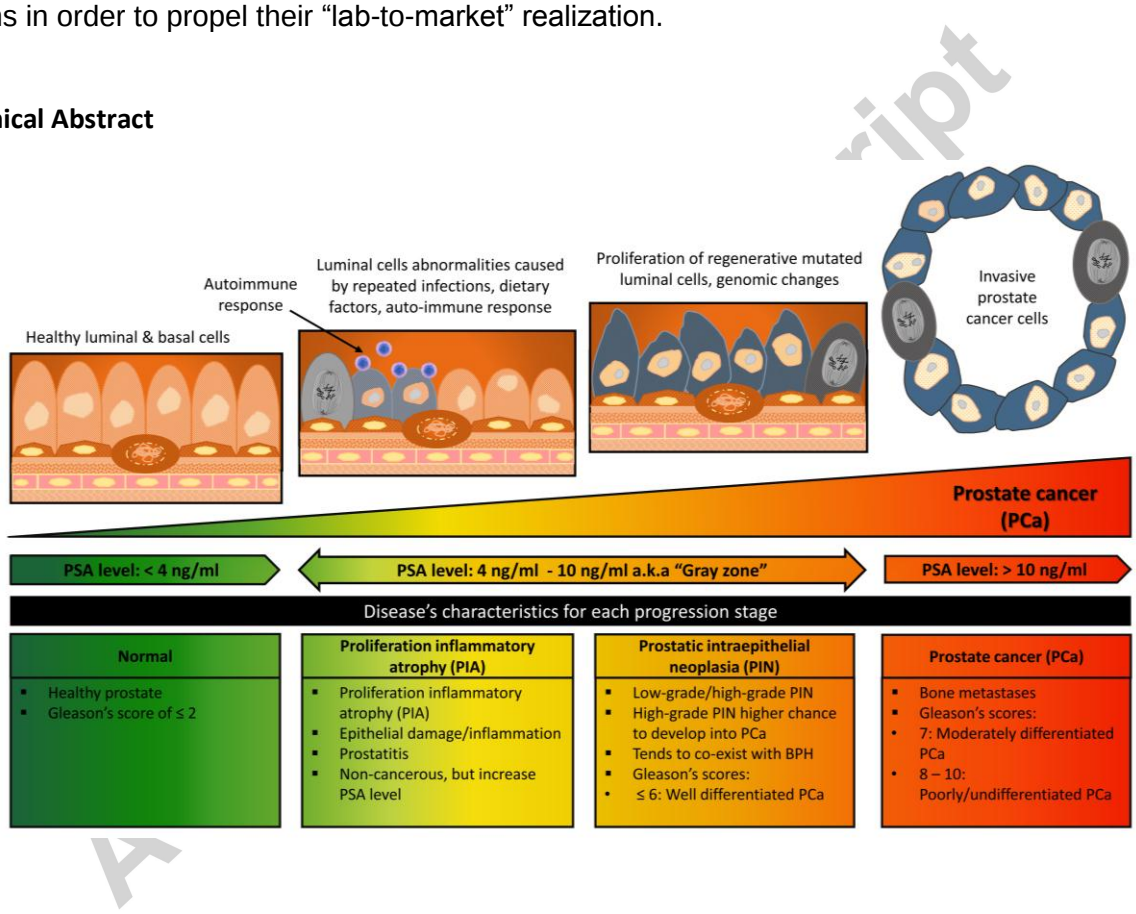

Abbreviations

Ag@MSN, silver hybridized mesoporous silica nanoparticles; AFP, alpha-fetoprotein; APBA, 3-aminophenylboroic acid; APTES, 3-aminopropyltriethoxysilane; APTMS, aldehyde propyltrimethoxysilane; AuNPs@GMCs, graphitized mesoporous carbon-gold nanoparticles; BSA, bovine serum albumin; BPH, benign prostatic hyperplasia; CAS-MWCNTs, cross-linked starch functionalized MWCNTs; CEA, carcinoembryonic antigen; Cys-SAM, cysteamine self-assembled monolayer; DPV, differential pulse voltammetry; EDC/NHS, N-ethyl-N'-(3-dimethylaminopropyl) carbodiimide/ N-hydroxysuccinimide; Fc, 6-ferrocenyl hexanethiol; fPSA, free Prostate-Specific

Antigen; GA, glutaraldehyde; HfO_2, hafnium oxide; HGPIN, high-grade prostatic intraepithelial neoplasia; HRP, horse radish peroxidase; HAS, human serum albumin; HSMs, hollow mesoporous silica microspheres; IL, ionic liquid; IL-6, interleukin-6; In_2O_3-NWs, indium (III) oxide nanowires; LGPIN, low-grade prostatic intraepithelial neoplasia; LSV, linear sweep voltammetry; MWCNTs, multi-walled carbon nanotubes; MU, 11-mercapto-1-undecanol; MUA, 11-mercaptoundecanoic acid; NPG, nano-porous gold; OPD, O-phenylenediamine; OTS, octadecyltrichlorosilane; PAMAM, Polyamidoamine dendrimer; p-AP, P-aminophenyl phosphate; PASE, 1-pyrenebutonoic acid succinimidyl ester; PB, 1-Pyrenbutanol; PCa, prostate cancer; PDDA, Poly (dimethyldiallyammonium chloride); PEG, Poly(ethylene glycol); PF-4, platelet factor-4; PGE, pyrolytic graphite electrode; Poly(1,2-DAB), Poly(1,2-diaminobenzene); PSA, prostate-specific antigen; PSA-ACT, alpha-1-anti-chymotrypsin prostate-specific antigen; PSMA, prostate-specific membrane antigen; PS-Fc, ferrocene incorporated polystyrene spheres; Pt, platinum; rGO, reduced graphene oxide; Streptavidin-AP, streptavidin-labeled with alkaline phosphatase; SWNTs, single-walled carbon nanotubes; SWV, square wave voltammetry; TH, thionine; tPSA, total Prostate-Specific Antigen

Keywords

Bioelectronic; biosensor; immunosensors; prostate cancer; prostate-specific antigen.

1. Introduction

"A very rare disease" was once an assuring description by J. Adams upon his first sighting on prostate cancer (PCa) in 1853 (Denmeade and Isaacs, 2002). Truth be told, nowadays, this rarity has diminished as PCa is now one of the most prevalent form of silent killers among men worldwide. Currently, PCa contributes up to 29% of all cancers cases, and accounts for 13% deaths (Pentyala et al., 2016). In 2008, global incidence of PCa was recorded at ~899,000 cases, and about ~29% (258,000 cases) died from the disease (Ferlay et al., 2010). Worth noting, approximately 14% (122,000) of the total worldwide incidences in 2008 were from Asia-Pacific region, with top-three cases include Japan (32%), China (28%), and Australia (15%) (Baade et al., 2013). Despite the lower incidence rate among Asian men compared to the Western countries, Asian men in general, has higher proportions to be diagnosed at advanced cancer stage (Ito, 2014).

PCa is a form of malignant neoplasms of the prostate gland which is highly prevalent among men of age 50 and older. Being rarely symptomatic, it grows silently and hardly detectable. Once presenting, it usually signifies localized proliferation or metastasis to nearby organs. Localized extension of cancer cells often results in urinary obstruction, irritative voiding symptoms, and further progression may affect the quality of sexual life. Bone tumor (Coleman, 2001), metastatic spinal cord compression (MSCC) (Walji et al., 2008), and osteoporosis (Bienz and Saad, 2015) are

among the fatal complications arise due to late-stage PCa metastatic. Prior to introduction of androgen-ablation therapy by Charles Huggins in 1940s, the metastasized cancer patients were succumbed to the disease within only 1 to 2 years (Denmeade and Isaacs, 2002).

Prior to the advent of prostate-specific antigen (PSA), the prostatic acid phosphatase (PAP) was first used before it was soon overshadowed by the inherent advantages of the PSA (Seamonds et al., 1986). PSA, or human kallikrein 3 (hK3 or KLK3) is the current gold standard serum marker for preoperative diagnosis, screening, and for monitoring post-treatment of PCa. PSA is a 33-kDa androgen-regulated serine protease of the kallikrein family that is produced in the ducts and acinar cells of the prostate. It liquefies seminal coagulum of the semen, thus plays a great role in men sexual health (Robert et al., 1997). The precursor for PCa detection is by monitoring the PSA concentration in the human serum. A healthy prostate normally leaks only a minute concentration into the circulatory system, typically at lower than 4 ng/ml, thus, 4 ng/ml is the internationally recognized threshold value for PCa occurrence. The diagnostic 'gray zone' of 4 ng/ml to 10 ng/ml is the high hit-and-miss region due to false-positive and false-negative diagnoses. In a separate study among Asian men revealed patients with PSA level of <4 ng/ml, 4 ng/ml to 10 ng/ml, and >10 ng/ml have respective likelihood for the cancer; 12.4% - 13.4%, 15.9% - 19.6%, 53.7% - 59.5%, respectively, in which is considerably lower as compared to the American counterpart; 10% - 21%, 25%, and 67% (Seo et al., 2007; Yang et al., 2006). The stages of PCa with respect to the PSA levels are well-depicted in **Fig. 1**. The serum PSA that leaks into the bloodstream exists in two forms; one that is bound predominantly to protease inhibitors to co-exist in complexed forms, i.e. alpha-1-antichymotrypsin (PSA-ACT) and alpha-2-macroglobulin (PSA-AMG), and the other exists in an unbound form, called free-PSA (fPSA). The complex forms (cPSA), i.e. PSA-ACT and PSA-AMG, exist in greater abundance in the PCa patients compared to the fPSA. Furthermore, a study shows the elevation of fPSA concentration within the 'gray zone' is more likely due to proliferation of benign prostatic hyperplasia (BPH) and prostatitis - a non-malignant form of inflammation on prostate wall, and not from the PCa (Catalona et al., 1995). Different PSA isoforms are reported may aid in differentiating PCa from benign disease, which include, a) using the -2 truncation proPSA form (Catalona et al., 2003; Mikolajczyk et al., 2004), b) by measuring the level of intact PSA (both mature and proPSA) and ratio of nicked PSA (cleaved to site Lys145 and Lys146) to total PSA (fPSA + cPSA) (Nurmikko et al., 2001; Steuber et al., 2005), and c) monitoring the cleaved BPSA level (Slawin et al., 2005). Since its first identification (Ablin et al., 1970) as well as discovery in 1970s (Wang et al., 1979), followed by the approval of the Food and Drug Administration (FDA) in 1984 (Murphy and Watson, 2012), PSA remains the most anticipated serum marker for PCa until today, albeit its associative controversies (Etzioni et al., 2002). PSA screening with conjunction of digital rectal examination (DRE) is more sensitive in detecting organ-confined PCa compared to DRE or TRUS (Brawer et al., 1992; Crawford et al., 1996; Mettlin et al., 1993) alone. It was reported the current estimated detection success rate is ~70-80%, and ~50% increase before the use of PSA (Catalona et al., 1993). Besides, (Hankey et

al., 1999) reported on strong evidence of PSA screening has led to a sustained decline in PCa mortality. Though, single serum PSA screening lacks specificity to PCa. It requires large sample studies, i.e. number of biopsies, to save just a single life (Stattin et al., 2015). Recent studies have improved on PSA specificity by means of combining the serum PSA testing with other kallikrein family markers and markers of RNA expression, as reported in (Rigau et al., 2011; Salami et al., 2013; Vickers et al., 2011). Hence, the PCa biosensors which allow for low sample volume, and simultaneous detection of multiple markers are very much needed.

An accurate diagnosis at earlier stages of cancer is crucial to yield better disease monitoring and successful treatment for PCa. Many conventional PSA detection methods have been developed, such as, enzyme-linked immunosorbent assay (ELISA) (Matsumoto et al., 2000, 1999), fluorescence immunoassay (Choi et al., 2013), bioluminescent immunoassay (Ito et al., 2007), chemiluminescence immunoassay (Jolly et al., 2016), and time-resolved fluorescence assay (Härmä et al., 2003; Siivola et al., 2000). Albeit their good sensitivity, these methods are complicated, require labels or tags, laborious, non-portable, time-consuming, and expensive. Another interesting method, the immunochromatography test strip (ICTS) (Li et al., 2014) offers the speed, portability, simplicity and point-of-care (PoC) testing, however it requires high antigen loading to produce translatable output. Furthermore, most of the reported ICTS outputs are of qualitative nature at most, and rarely semi-quantitative. Developing high-performance sensors can overcome these limitations, and hence, recent attentions on developing the one-step-ahead bioelectronic immunosensors hold the unprecedented promises for PCa detection. Bioelectronics can be broadly defined as the merger of electronics with biological molecules, where a bioelectronic device transduces signal from the biomolecular interaction to electrical signals at the system interface (Zhang and Lieber, 2016). It offers significant advantages in manufacturability and compatible with complementary metal-oxide-semiconductor (CMOS) technologies, ease to use and better throughput compared to label-based approach. Bioelectronics can be amperometric, voltammetric, potentiometric, conductometric, impedance, or field effect and may be based on oxidation/reduction reactions (Huang et al., 2015).

Owing to these exuberant progresses, this review aims to elucidate the recent advancement in bioelectronic immunosensors for the detection of PSA biomarker. The paper emphasizes on reviewing the sensing device's architectures and principles, sensing materials and surface modifications techniques, biomolecular immobilization and surface binding strategies, also, the sensing performances of the reported assays. Finally, discussing on the future of the sensor's technology based on the current research trends, further, concludes on the author's perspectives toward the direction of research's propagations.

2. Field-Effect Transistors-Based Bioelectronics

Field-effect Transistor (FET) was first demonstrated as switching devices by D. Kahng and M. Atallah in 1960. Traditionally, FET consists of source and drain separated with channel in between, fabricated on a substrate. The device uses the variations in electric field potential on the gate electrode to control the conductivity of the source and drain terminals. Ten years later, Bergveld demonstrated the first transistor-based biosensors known as Ion-Selective Field Effect Transistor (ISFET) in 1970 (Bergveld, 1970). He demonstrated the measurement of current as a function of Na+ ions solution with a constant pH value. The device is fabricated on the glass substrate, based on three electrode system i.e. Ag/AgCl as a top-gate electrode, drain and source electrodes. Since then, FET have attracted a significant interest among researchers due to its label-free, real-time and sensitive detection of biomolecules properties. In addition, FETs biosensors enable the diagnostic information to be conveyed rapidly, simply, in low-cost fashion. Besides, it holds unprecedented potentials to fulfill the demands for the portability of point-of-care (PoC) devices. More complexity in architecture can also be demonstrated with the presence of additional back-gate bias to enable 4-electrodes system i.e. Ag/AgCl, source, drain and back-gate terminals, with the aims to improve the sensitivity of detection. **Fig. 2** illustrates the typical device structure of a 4-electrodes FET-biosensor and the common transducers' surface modification techniques for biosensing amplification strategies. The inset 2(a) depicts the structure of 4-electrodes FET-biosensor with drain, source, Ag/AgCl electrode, and back-gate terminals that enable for ambipolar switching conduction, integrated onto PDMS microfluidic delivery system for a controlled sample analyte delivery onto the biosensing surface. Inset 2(b) shows the biosensing sensitivity enhancement techniques through the modifications of the biosensors' transducers by the implementation of zero-dimensional (0D), one-dimensional (1D), and two-dimensional (2D) materials.

FETs based biosensors are the device of choice to detect biological molecules in electrolytic (Wang, 2006) or dry environments (M. Nuzaihan et al., 2016). Given a sufficient potential on the drain-source terminals to drive the electrons, the control of this electric field potential on the gate would either attract or repel the charge carriers in the conduction channel, thus controlling the on- or off- state of the device. On the other hand, in the FET biosensors however, the controls of gate's electrical field potential rely on the well-known "gating-effect" mechanism, which uses the charge of biomolecules or polar biological species, to gate the current through the transistor's drain and source terminals. To realize this, the metal gate electrode in a traditional transistor is typically replaced by a transducer material that is reactive towards the biomolecular changes on its surface, in which the transducer-biomolecules interactions are induced by the analyte solution. The main drawback of FETs-based biosensors is the effect of ionic screening to the sensitivity and limit of detection (LOD) due to large molecules adsorption on the transducer surface. The integration of zero-dimensional (0D) nanoparticles e.g. AuNPs, AgNPs, one-dimensional (1D) nanostructures e.g.

nanowires, nanotubes, nanorods and also two-dimensional (2D) nanomaterials e.g. graphene-based materials, molybdenum disulfide were reported to have drastically improved these characteristics due to increased surface-to-volume ratio. Besides that, the use of antigen binding fragment (Cheng et al., 2014) which has smaller molecular size was reported to yield higher sensitivity and wider concentration range by using the FET device. Switching polar conduction (i.e. unipolar and ambipolar conduction due to additional gate biasing) induces higher sensitivity of the device by manipulating the distribution of electron/holes carriers in the substrate (Zhang and Lieber, 2016). With ambipolar conduction, the device's sensitivity and LOD can be improved, allowing for detection of low concentration of biomolecular species.

2.1 Nanowire Field-Effect Transistor (NWs-FET)

In the form of 1D structure of nanowire, NWs-FET offers large surface-area-to-volume-ratio which makes it an excellent choice for highly sensitive biomolecules detection. The fabrication and characterization of nanowire can be realized by either top-down or bottom-up approaches. Top-down technique involves lithography, deposition and etching steps which offer better controlled of the developing nano-structures, but with an expense of high processing complexity and luxurious equipment. On the other hand, bottom-up technique involves synthesizing the target nanostructures from single atoms and molecules, with key nanometer-scale metrics built in through synthesis, thus enabling for smaller synthesized nano-structures. Both approaches have been well-reviewed (Chen et al., 2011; Zhang and Lieber, 2016; Zhang and Ning, 2012). Silicon nanowire is interesting due to the fact that silicon is a matured semiconductor material and has been widely used in today's electronic devices. The main advantages include its characteristics can be easily modified with impurities, in addition to low-cost raw material.

Huang et al. (Huang et al., 2013) demonstrated a highly sensitive femto-range limit-of-detection (LOD) of PSA protein by developing an n-type poly-Si NWFET immunosensors assay. The team integrated the poly-SiNW with polydimethylsiloxane (PDMS) microfluidic system for sample handling and fluidic manipulation which allows for improved transport of analyte onto the bio-recognition element of the sensing system. The poly-Si nanowires were fabricated on multi-layered silicon substrate-oxide-silicon nitride-TEOS oxide through layer-by-layer (LBL) assembling surface modification with poly-Si NWs, APTES, glutaraldehyde, and anti-PSA MAb probe. The silicon substrate-oxide-silicon nitride stacked layer was reported preventing the liquid invasion phenomenon and maintaining an excellent electrical characteristic in the tested aqueous solution (Hsiao et al., 2009; C. H. Lin et al., 2009). The acclaimed implementation of sidewall spacer technique reported earlier by Lin et. al. (C. H. Lin et al., 2009) gives the advantages of simplicity and low cost compared to electron beam lithography. Employing the label-free I-V measurement to detect the current changes across drain-source terminals due to biomolecular bindings ("gating-effects"), the sample analytes with constant flow rate of 83 µL/min were conveyed onto the poly-Si

NW-FET transducer surface through the microfluidic system with reported linear detection range of 500 pg/mL to 5 fg/mL of PSA concentrations in both 0.01x PBS buffered solutions and in desalted human serum. Presnova et al. (Presnova et al., 2017) reported on the application of symmetric half fragment anti-PSA, fragmented in the 2-mercaptoethylamine (2-MEA) as a reducing agent, then conjugated to AuNPs for signal amplification. The silicon NWs-FET was functionalized with 3-glycidopropyltriethoxysilane-thiol group conjugates (GOPS-SH), then immobilization of half-fragment anti-PSA was done through the thiol-AuNPs reaction. The sensor's performance on detection of PSA was performed in diluted serum at 1/100 with 0.01 x PBS pH 8.0, resulting in linear detection range of 500 ng/ml – 23 fg/ml (CV: 0.97).

Zheng et. al. (Zheng et al., 2005) developed and reported on integrated immunosensors assay which enables for simultaneous detections of fPSA, PSA-ACT, CEA, and mucin-1 antigens through a highly sensitive multiplexed Si-based NWFET arrays, shown in **Fig. 3**. The transducer-surface-linked MAb receptors were immobilized onto each of the distinct nanowires array by first treating the Si-NW with aldehyde propyltrimethoxysilane (APTMS), followed by the MAb receptors (anti-PSA/anti-ACT-PSA/anti-CEA/anti-mucin-1) which were covalently bound onto the aldehyde-terminated NWs surfaces. By employing a label-free, real-time electrical-based approach by simultaneously measuring the conductance change over time during the Ab-Ag binding, the group has reported the detection limit of 0.9 pg/ml in undiluted serum samples and concentrations limit of 75 fg/ml in PSA, 100 fg/ml in CEA, and 75 fg/ml in mucin-1 in buffered solutions with a signal-to-noise ratio (SNR) higher than 3. The team also demonstrated a method for simultaneous discrimination against false-positives detection that renders the device to be essentially 100% selective (Patolsky et al., 2007).

2.2 Carbon Nanotubes Field-Effect Transistor (CNT-FET)

Carbon nanotubes (CNTs) are novel molecular nanowires with metallic or semi-conducting nanotubes, commonly available in two novel forms; single-walled nanotubes (SWNTs) and multi-walled nanotubes (MWNTs). The high surface area of conductive SWNTs, estimated up to 1600 m^2/g provides an excellent platform for the attachment of high densities of capture antibodies to enhance the biosensing performance. The ballistic electronic conduction along the length axis of SWNTs with current density approaching 10^9 A/cm^2 can improve the sensor performance (Kim et al., 2007).

Kim et al. (Kim et al., 2009) reported on the enhancement of sensitivity and specificity of their SWNT-FET by investigating the effects of varying the linker-to-spacer ratios on the detection of PSA-ACT complex serum, as shown in **Fig. 4**. By implementing a label-free, real-time electrical measurement (conductance changes across the drain-source of SWNT over time, as the platinum, Pt-reference electrode as gate terminal is biased), the team investigated on the optimal ration of 1-pyrenebutanoic acid succinimidyl ester (PASE) which acted as the linker and 1-Pyrenbutanol (PB) as the spacer. By employing the SiO_2-methyl-terminated OTS SAM-SWNTs-PASE(linker)-

PB(spacer)-PSA-ACT MAb as surface modification technique, the team reported the 1:3 ratios of PASE: PB resulted in an optimal detection limit of PSA-ACT complex concentration down to 1.0 ng/ml without any pre-treatment, compared to about 500 ng/ml LOD without linker/spacer. The research team further noted the advantage of the linker and spacer used was able to suppress the non-specific binding of the non-target proteins. The spacer employed in the research has been reported to enhance the sensitivity of the CNT-FET device, besides, simplifying the pre-treatment process for the use of the PSA-ACT's capture antibody.

Li et al. (Li et al., 2005) reported on novel electrochemical immunoassay by integration of n-type In_2O_3- SiNWs with p-type SWCNTs biosensor for a complementary detection of PSA serum. The research team introduced a novel methodology to covalently bind anti-PSA onto the In_2O_3 NWs through the onsite surface synthesis of a succinimidyl-linking molecule. Electrical characterization by I-V electrical measurement of the SiNWs/SWNTs hybrid assay revealed a complement response between the SiNWs and SWNTs due to the nature of the doping types of the device; n-type SiNWs and p-type SWNTs. The device was tested by incubating the device into PBS-buffered PSA solution down to 5 ng/ml on the SiNWs, and 50 ng/ml on the SWNTs. The group reported a SNR of about 20 for the SiNWs detection, which translate a detection limit of about 250 pg/ml from the device. The group reported to be working on testing the device under different PSA concentrations, though we have not found any of the findings published. In a different work, Okuno et al. (Okuno et al., 2007) demonstrated on an assay for tPSA detection limit down to 0.25 ng/ml using SWCNTs-modified platinum (Pt)-microelectrodes as the working electrode (WE), Pt wire as the counter electrode (CE), and Ag/AgCl as the reference electrode (RE) in the Differential Pulse Voltammetry (DPV) measurement setup. The biological recognition event took place on the functionalized microelectrodes by realizing the following immobilization strategy; SiO_2 substrate – Pt-microelectrodes – SWCNTs – PASE - anti-tPSA MAb – tPSA binding.

A single protein based immunoassay detection for PSA often suffers from limitation in the specificity for predictive ability of PCa. Chikkaveeraiah et. al. (Chikkaveeraiah et al., 2009) successfully reported on a horseradish peroxidase, (HRP)-labelled immunoarray-based SWCNTs forest for simultaneous detection of PSA, PSMA, PF-4, and IL-6 proteins in clinical human serum samples of PCa patients. By employing a sandwich-type surface binding technique of Pt – SWCNTs - EDC/NHS - anti-Ab_1 (anti-PSA, anti-PSMA, anti-PF-4, anti-IL-6) - Ag (PSA, PSMA, PF-4, IL-6) - Ab_2-conjugate, the amperometric-based detections of all antigens were demonstrated with LODs of PSA: 1 ng/ml, PSMA: 10 ng/ml, PF-4: 1 ng/ml, and IL-6: 0.03 ng/ml respectively. Linear detection ranges were reported at 1-40 ng/ml for PSA, 10-250 ng/ml for PSMA, 1-40 ng/ml for PF-4, and 50-500 pg/ml for IL-6. All tests were conducted at physiological concentration ranges, by measuring the amperometric responses of the electrochemical over the electrocatalytic reduction behavior of HRP-label towards hydrogen peroxide, (H_2O_2) in hydroquinone mediator.

2.3 *Molybdenum Disulfide (MoS_2) Functionalized ISFET*

The advancement in materials science and the demanding world of biosensors with a new, better transducing material have attracted attention on molybdenum disulfide (MoS_2), due to its 2-dimensional (2D) atomically layered structure. Unlike the 2D graphene material which lacks bandgap, direct energy bandgap of MoS_2 (Mak et al., 2010) results in a lower leakage current of the device. Interested readers may find this review on MoS_2 (Kalantar-zadeh and Ou, 2016) useful. MoS_2 based biosensors have the potential to be a mainstream in the world of immunoassays due to the growing research works to synthesis the 2D MoS_2 on a large surface area using chemical vapor deposition (CVD) (Liu et al., 2012; Zhan et al., 2012). Naylor and co-workers (Naylor et al., 2016) have recently reported on a CVD-grown MoS_2 monolayer on FET transducer as opioid biosensor. Another MoS_2 based pH sensor also reported by Sarkar and co-workers (Sarkar et al., 2014) was able to detect a wide pH 3 to pH 9 range, at more than 74-fold higher sensitivity than graphene-based sensors.

The publications on the use of MoS_2 for PCa detection are still preliminary, but is gaining considerable attention. Wang et al. (Wang et al., 2014) functionalized a multi-layer MoS_2 nanosheet on a high-κ HfO_2 as gate dielectric, and employed the APTES –GA –anti-PSA MAb as the immobilization strategy for a sensitive, label-free I-V electrical-based detection for serum PSA dilution down to 375 fM. The team demonstrated a successful microfluidic integration for sample delivery as well. The lab-on-a-chip (LoC) system was tested to exhibit favorable binding specificity through effective BSA discrimination at tested concentration of 1 µg/ml. However, the hydrophilic surface property of the HfO_2 dielectric resulted in a low affinity to biomolecules adsorption. A separate work done by Lee and colleagues (Lee et al., 2014) as depicted in **Fig. 5**, reported on a direct anti-PSA immobilization onto a dielectric-free, hydrophobic MoS_2 thin film surface to yield higher affinity of protein-surface adsorption onto the transducer. The inset a(i) shows the schematic illustration of the MoS_2 functionalized dielectric-free transducer in between the source and terminals of the device. Meanwhile, inset a(ii) shows the 3D AFM topography revealing ~80 nm MoS_2 thin film on the sensing area. On the other hand, the approach to eliminate the HfO_2 gate dielectric has greatly improved the hydrophobicity on the sensing surface, as witnessed in the water contact angle measurement of 75.77°, shown in the inset 5(b). This strategy has greatly benefited its measured label-free I-V electrical performance, reported in Fig. 5c. The inset c(i) shows the respectable I_d-V_{gs} transfer characteristics of the immunosensor for immobilized 100 µg/ml of anti-PSA bound to the PSA antigens at concentration ranging from 1 pg/ml – 10 ng/ml. The application of the back-gate ambipolar conduction, as reported in the inset c(ii), shows excellent linearity in the I_d-V_{ds} responses, when tested under the immobilized antibody concentration of 100 µg/ml, back-gate bias effect, V_{gs} of -32 V to 0 V, in 8 V steps. The inset c(iii) revealed a ~10-fold reduction in I_d-V_{ds} output response, in which translates to ~10-fold of current amplification, when tested at fixed PSA antigens concentration of 10 ng/ml, under back-gate bias

of -32 V to 0 V. The demonstrated strategy further revealed a LOD of 1 pg/ml by the application of off-current electrical measurement technique.

3. Customized-Electrodes Devices-Based Bioelectronics

In addition to the field-effect transistors-based method, customized-electrodes devices-based method is another interesting architecture that is gaining much attention among the researchers in biosensing applications. The first demonstration of this type of biosensor was reported by Bergveld (Bergveld, 1991). Since then, various device architectures can be found in the literatures such as interdigitated electrode (IDE), screen-printed electrode (SPE) or glassy carbon electrode (GCE), as illustrated in Fig. 6. In the figure, Fig. 6a represents the typical customized-electrodes devices-based structures. The inset a(i) shows the optical images of interdigitated electrodes (IDE) for biosensing, a(ii) shows screen-printed electrode (SPE)-integrated immunochromatographic electrochemical biosensor (IEB), and a(iii) shows surface functionalization of a glassy carbon electrode (GCE) substrate. Meanwhile, Fig. 6b depicts the commonly implemented electrochemical detection techniques in customized-electrodes devices-based setup. The inset figures show the outputs for each of the detection techniques, namely b(i) differential pulse voltammetry (DPV), b(ii) square wave voltammetry (SWV), b(iii) cyclic voltammetry (CV), and b(iv) electrochemical impedance spectroscopy (EIS). The customized-electrodes devices-based structure consists of substrate materials (i.e. glass, polyvinyl-chloride, ceramic, silicon) with insulating layer (typically glass, air), and are separated with conducting (i.e. gold, platinum, silver/palladium alloy) or semiconducting (i.e. graphene-based, carbon) electrodes. The presence of insulator and conductor/semiconductor in between the electrodes represent the capacitance principle, which can be arranged either horizontally or vertically. The sensing area can be deposited with thin films deposition (i.e. graphene, metals oxide), nanoparticles (typically AgNPs, AuNPs), and nanostructured layers (i.e. CNTs, NWs, nanorods) for further modifications and biological immobilization. These assays are well-complemented in the world of portable biosensors, covering the diverse field of applications, e.g. health and food safety, including the detection of Ochratoxin A (Malvano et al., 2016), acetic acid (Ndiaye et al., 2016), *Escherichia coli* (L. Wang et al., 2015), antibiotics in milk (Davis and Higson, 2010), viruses in plasma and saliva (Shafiee et al., 2015); for environmental monitoring: water quality (Zen et al., 2002), nitrite (C. Y. Lin et al., 2009), pesticides (Arduini et al., 2006; Kumar and D'Souza, 2011; Otero et al., 2011), cadmium (Zaouak et al., 2010), mercury ions (Bernalte et al., 2011), arsenic (Sanllorente-Méndez et al., 2010, 2009), gas pollution (Mbarek et al., 2007; Morata et al., 2007); and photovoltaic solar cells (Small et al., 2011). Simple, rapid, sensitive, portable, low cost, and mass-reproducible are the main attributes of these types of biosensors that may underpin the successful route from LoC to "lab-to-market" status.

3.1 *Interdigitated Electrodes (IDE)*

IDE consists of a series of parallel electrodes connected together and separated to alternating interlocked electrode by insulators, forming a set of interdigitated fingers. The detection mechanism of IDE sensors is based on the changes in the dielectric constant, caused by the binding event of target molecules to receptors (antibodies, DNA, proteins, and other bio-recognition elements) immobilized on the surface of the electrodes. Higher sensitivity can be achieved by 1) the use of IDE arrays to increase the active area for the binding events, and 2) the reduction in the distance between the finger electrodes. However, tighter finger electrodes are known to require costly and time-consuming processes, e.g. e-beam lithography method. Alternately, higher sensitivity can be achieved with deposition on nanoparticles between the finger electrodes of an IDE, which is able to shorten the distance between these fingers. In an electrical aspect, IDE is an interesting device architecture, with the presence of small amplitude sinusoidal excitation signal. The measurement of IDE sensors is not only limited to capacitance measurement (due to presence of gap in between the electrodes) but also can be extended to electrochemical impedance spectroscopy (EIS) sensors (Guan et al., 2004; Lisdat and Schäfer, 2008). In EIS, the changes of electrical properties on the surface can be represented by an equivalent circuit to signify the different physiochemical properties (Lisdat and Schäfer, 2008), related to the charge transfer processes, in which both R&C are frequency dependent (Berggren et al., 2001). EIS-based IDE offers additional advantages of improved sensitivity, rapid kinetics, increased signal-to-noise (SNR) ratio and large electrode aspect ratio (W/L) (Arya and Bhansali, 2012).

Chornokur et al. (Chornokur et al., 2011) showed that micron-scale IDE structure is possible for sensitive detection of PSA down to 1 pg/ml of LOD, with reported linear detection range of 1 pg/ml to 100 pg/ml. The IDE device was fabricated using photolithographic technique with digit width of 5 μm, 3200 μm long, and distributed over 5500 μm in length with spacing of 10 μm between each inter-digit. Using gold deposited electrode to enhance devices' sensitivity, the transducer surface was modified with dithiobis(succinimidyl propionate) (DTSP) self-assembled monolayer (SAM), followed by immobilization of anti-PSA MAb. The surface modification's characterization was observed using the EIS technique to measure the changes in the IDE electrodes impedance through the Nyquist plots in the ferricyanide/ferrocyanide ($Fe(CN)_6^{3-/4-}$) redox probe solution during the immobilization and Ab-Ag binding processes. The devices' selectivity was tested in different concentrations of anti-cortisol MAb for non-selective binding (NSB) test, which resulted in favorable selectivity of the device. A separate work of the same group (Arya and Bhansali, 2012) revealed an improved linear detection range from 1pg/ml to 100 ng/ml by using Cysteamine-SAM to replace the DTSP-SAM as the linker to immobilize the anti-PSA on the identical Au electrode surface. The similar EIS measurement setup was used to measure the impedance changes in the $Fe(CN)_6^{3-/4-}$ redox probe solution. Huang et al. (Huang et al., 2009) also reported on a micro-gapped interdigitated electrode array (MGIDEA) using the enzymatic silver deposition approach for an

enhanced sensitivity for the detection of PSA. The device has digit width of 80 µm, 3000 µm long, and consists of 18 digits with 80 µm gap, and the surface modification was based on the sandwiched-based immunoassay; Ti-Au bilayer – APTES – GA – anti-PSA140 mAb – PSA – anti-PSA103 mAb-alkaline phosphatase (ALP) conjugate – Ag deposit. The electrochemical measurement was performed using the linear sweep voltammetry (LSV) technique (potential range from 0 – 50 mV, scan rate of 1 mV/s at 1 mV internal) to plot the I-V responses on the functionalized MGIDEA electrodes for different concentration of PSA. With a reported linear detection range of 1.0 pg/l to 1.0 µg/l and detection limit of 0.9 pg/l, this device demonstrates a promising platform for high sensitivity PSA detection using the IDE electrodes approach.

3.2 Screen-Printed Electrodes (SPE)

Barton et al. (Barton et al., 2008) reported on the polyalinine (PANI)-modified carbon-SPE based electrochemical sensor. The author demonstrated two immobilization strategies, firstly through the avidin-biotin affinity reaction, and secondly, through the anti-PSA probes entrapment during PANI electro-polymerization process. The detection of different concentrations of PSA were carried out using the alternating current (AC) impedance measurement technique, from 1 Hz to 10 kHz in the pH 7.4 phosphate buffer (PB) containing a 50:50 mixed ratio of $Fe(CN)_6^{3-/4-}$ at 10 mmol/L concentration as a redox mediator. It was found that the affinity reaction strategy resulted in a LOD of 1 pg/ml (linear detection range: 1 pg/ml – 100 pg/ml), meanwhile, the entrapment strategy yielded a LOD of 1 ng/ml (linear detection range: 1 ng/ml – 200 ng/ml). Escamilla-Gomez et al. (Escamilla-Gomez et al., 2009) have achieved a linear detection range of 10 ng/ml to 100 ng/ml for both fPSA and tPSA by developing an immunosensor device through surface modification on the screen-printed carbon electrode (SPCE) and screen-printed gold electrode (SPGE). The team also reported on novel dual-sensor design for simultaneous detections of both fPSA and tPSA using the gold modified screen-printed carbon dual sensor (*Dualsensor-nAu).* The device was reported to be able to detect the fPSA/tPSA at a linear detection range of 1 ng/ml to 10 ng/ml, by using the cyclic voltammetry (CV) electrochemical detection technique. Lin et al. (Lin et al., 2008) have optimized a portable immunochromatographic electrochemical biosensor (IEB-LoC) using a disposable SPE for sample delivery. By requiring serum PSA sample size of 100 ul, the team reported a linear detection range of 0.05 ng/ml – 4 ng/ml under the tested standard serum PSA samples of 0 ng/ml to 4 ng/ml (by 20-fold dilution with PBS buffer) and a detection limit of 0.02 ng/ml. Another LoC, a novel vegetable parchment (VP)-based SPEs as transducer platform has been reported by Yan et al. (Yan et al., 2012). Through amine-functionalized graphene ($GR\text{-}NH_2$), the anti-PSA probe was immobilized using the GA linker. The devices' sensitivity and conductivity was amplified by the conjugation of HRP-anti-PSA complex and AuNPs. The LoC immunosensor required a low serum PSA sample of 10 µm, conveyed through the chromatography paper-based microfluidic channel with a reported linear detection range of 0.002 ng/ml – 2.0 µg/ml and LOD: 0.46 pg/ml (SNR =3).

The implementation of recombinant single-chain antibody (scAb) was reported by Zapatero-Rodríguez et al. (Zapatero-Rodríguez et al., 2017). The expression of scAb was reformatted from the chicken recombinant anti-fPSA single-chain variable fragment (scFv) B8. The sandwich-based immunoassay for fPSA detection strategy consists of the immunomagnetic separation (IMS) of fPSA from the sample using anti-fPSA scAb-magnetic particles (MPs) conjugates, and then followed by the immunorecognition of captured fPSA by the pre-incubated HRP-labelled anti-PSA Ab_2 conjugates, using the amperometric measurement in PBS buffer. The surface functionalization strategies on the carbon SPE can be summarized as MPs-anti-fPSA scAb conjugates – fPSA – HRP-labelled anti-fPSA Ab_2 conjugates. The assay was reported to yield a linear detection range up to 10 ng/ml, and a LOD of 0.5 ng/ml, dynamic range of detection of fPSA of 10 ng/ml (R^2 = 0.9979), and coefficient of variation was reported to be 8 – 12%. In a different study, Spain et al. (Spain et al., 2016) used the scFv clone B8 anti-PSA, which was conjugated with the electrocatalytic platinum nanoparticles (PtNPs) for PSA detection using the EIS technique. The assay yielded a linear detection of 30 ng/ml – 1 ng/ml, and LOD of 0.03 ng/ml. However, these studies require the extended performance tests in the physiological conditions in order to evaluate their real clinical values.

3.3 Glassy Carbon Electrode (GCE)

Salimi et al. (Salimi et al., 2013) implemented the ionic liquid, (IL)-MWCNTs nanocomposite based biosensor for detection of PSA. The surface modification was realized by mixing 10 µl of IL, 1-buthyl-methylpyrolydinium bis (trifluoromethyl sulfonyl) imide $[C_4mpyr][NTf_2]$, with 3 mg of CNTs, casted onto GCE surface to form the GCE-IL-MWCNTs nanocomposite. Thionine, (TH) was used as redox system for electrochemical probe. The immobilization of the anti-PSA on the CNTs transducer was in sandwich-type complex immunoassay. The complete binding strategy of the assay was GCE-IL-MWCNTs- anti-PSA MAb_1-PSA-anti-PSA MAb_2 conjugated HRP label. The primary anti-PSA was immobilized on the transducer through entrapment in the fabricated nanocomposite. The cyclic voltammetry based assays measurement principle reported a detection limit of PSA concentration as low as 20 pg/ml at signal-to-noise-ratio (SNR) >3. The reported detection assay took advantage of its' simple one-step fabrication method, high detection sensitivity of 0.95 µA ng/ml, good stability and reproducibility. The team reported the devices' detection coefficient of variations (CVs) of 2% and 1.35% at 5 ng/ml of PSA concentration, which were tested for five replications. Yang et al. (J. Yang et al., 2015) enhanced the detection limit using a similar MWCNTs by synthesizing AuNPs onto the CNTs transducer to amplify the devices' sensitivity response. Instead of employing the antibody entrapment in nanocomposite technique used by Salimi et al., Yang et. al took advantage of the EDC/NHS activations for covalent binding of the AuNPs-synthesized primary antibody onto the MWCNTs transducer surface. In contrast to physical entrapment, covalent binding technique by linking an activated functional groups was reported to improve the immune-sensors' performance (Masereel et al., 2011; Wilson and Nock,

2002). Yang et al. demonstrated an improved linear range of detection of tPSA from concentration of 100 ng/ml to 10 pg/ml, and an improved detection limit down to 5.4 pg/ml. On the other hand, Tian et al. (Tian et al., 2012) reported the use of cross-linked starch (CAS) for immobilization of AuNPs-conjugated anti-PSA onto the MWCNTs-deposited transducer surface. The reported linear ranges of detection of PSA concentrations were 3.0 ng/ml to 0.5 ng/ml and 0.5 ng/ml to 0.01 ng/ml, and a lowest detection limit of 7.0 pg/ml at SNR =3. The use of biocompatible CAS ensures good retention of nano-structural integrity and electrical properties of the nanotubes.

Y. Wang and colleagues (Y. Wang et al., 2015) used the high-molecular-weight silk peptide (10 kDa to 15 kDa) to functionalize the rGO nanosheet on the GCE surface to immobilize the anti-PSA probe. The silk peptide (SP) – rGO nanocomposite was first synthesized using the Hummers method (Hummers and Offeman, 1958), with the following modifications as shown before (Kovtyukhova et al., 1999). The synthesized SP – rGO nanocomposite, together with the anti-PSA were mixed in phosphatase buffer, subsequently dispersed onto the polished GCE surface and dried at 4 °C. The modified surface was then treated with GA vapor to stabilize the GCE/rGO-SP-anti-PSA through covalent cross-linking between the amino groups in anti-PSA epitopes and the SP, with the aldehyde of the GA. Using the BSA to block the unspecific binding, the selective binding of anti-PSA and serum PSA was characterized by CV and EIS measurements in hexacyanoferrate redox system using the potassium ferricyanide, $K_3[Fe(CN)_6]$/ $K_4[Fe(CN)_6]$ electroactive probes, reporting tested linear detection range from 0.1 ng/ml to 5.0 ng/ml and 5.0 ng/ml to 80.0 ng/ml. As for LOD, recorded at SNR=3 was down to 53 pg/ml. Similarly, another simple, direct assay as demonstrated by H. Wang et al. (Wang et al., 2013) used the mesoporous silica nanoparticle (MSN) to take advantage of its large surface area as an electrode material, functionalized onto the GCE surface. By hybridizing the MSN to the AgNPs according to literature (Zhao et al., 2009), the Ag@MSNs byproduct provides a combination of an enhanced electrical properties from the AgNPs, and a higher fixation for anti-PSA immobilized sites on the electrode from the high surface area of the MSN. By dispensing 6 µl Ag@MSNs and dried, the modified electrode was then treated with 2.5% GA solution. By treating with 5 µl human serum PSA and incubated for 1 hour, the team reported a detection range from 0.05 ng/ml – 50 ng/ml and a LOD of as low as 15 pg/ml (SNR = 3). Both works demonstrated their corresponding assays to yield good binding selectivity, detection reproducibility and stability, acceptable analytical reliability when compared to ELISA reference values.

The use of modified polymeric ferrocene (Fc) as the electrochemical label for PCa detection has been reported by Ding and teammates (Ding et al., 2013) by employing sandwich-type immunoreaction of GCE/GO-(EDC/NHS)-anti-PSA MAb_1/PSA/ anti-PSA MAb_2-(chitosan)/PS-Fc label. The GO preparation was also according to Hummers method (Hummers and Offeman, 1958), with modifications described by McAllister et al. (McAllister et al., 2007). Fc is widely used as an electrochemical label, as in (Le Floch et al., 2005; Rahman et al., 2009) due to its excellent

reversibility of redox activity and other attributes (Metzler-Nolte and Salmain, 2008). However, Fc-based electrochemical sensors often suffer from performance degradation due to its leakage from electrode surface. The group therefore, demonstrated a linked Fc to a polymeric derivative i.e. polystyrene spheres (PS) as the redox label to overcome this limitation. The PS – Fc conjugate was synthesized based on literature (Paine, 1990). The reported 'stripping voltammetry' assay was tested by measuring the cyclic voltammetry (CV) and square wave voltammetry (SWV) responses when the Fc label was 'stripped' from the PS – Fc conjugate by subjecting to tetrahydrofuran (THF). A linear detection range of PSA concentration from 20 ng/ml to 0.01 ng/ml and LOD of 1 pg/ml was reported.

Simultaneous detection of AFP and PSA via sandwich type immunoreaction was reported by Zhao et al. (Zhao et al., 2015). The primary antibodies (anti-AFP and anti-PSA) were linked by rGO-AuNPs conjugated on a modified GCE, then incubated in AFP and serum PSA for 50 min at 37°C to form immunocomplex. The redox labels, Azure A for AFP detection and Fc for PSA were bio-conjugated as follows: Azure A@anti-AFP Ab_2/Si@AuNPs and Fc@anti-PSA Ab_2/Si@AuNPs. Employing the DPV technique, the immunosensor in 1.0 mM of $Fe(CN)_6^{3-/4-}$ redox probe solution was reported to yield an ideal detection range of 0.01 ng/ml to 25 ng/ml for AFP and 0.012 ng/ml to 25 ng/ml for PSA. At SNR=3, the LODs were reported at 3.3 pg/ml for AFP and 4.0 pg/ml for PSA, respectively. The device was reported to exhibit acceptable selectivity, reproducibility, and stability for application in clinical analysis. Another sandwich-type immunoassay was demonstrated by Wu et al. (Wu et al., 2012) by using the nanoporous gold (NPG) to immobilize the primary anti-PSA via amine-Au affinity reaction. The secondary anti-PSA was labelled by hollow mesoporous silica microspheres (HSM) using the following conjugation strategy: anti-PSA MAb_2 – HRP – TH – HSMs. The group reported a linear detection range of 0.01 ng/ml to 10 ng/ml and LOD of 6.0 pg/ml with good reproducibility and stability.

Recent report on the application of peptide-based biosensing has garnered much attention. Tang et al. (Tang et al., 2017) has showed the use of specific peptide sequence (i.e. CEHSSKLQLAK-NH_2), demonstrated in amperometric biosensor has notably reported an impressive detection of linear concentration of PSA serum from 100 ng/ml down to 1 fg/ml, the lowest LOD reported in this review. Besides, the assay yielded excellent repeatability, detection specificity, stability and reliability.

4. Aptasensing Rivals Immunosensing

Aptamers are short, customizable single-stranded DNA or RNA-based oligonucleotides with high predilection to various small molecules, large proteins (Tombelli et al., 2005) and cells (Estévez et al., 2010; Soontornworajit and Wang, 2011). Their binding nature with target molecules relies on the combination of van der Waals surface contacts, hydrogen bonds, stacking interactions, electrostatic and hydrophobic interactions (Citartan et al., 2012; Gopinath, 2011). These high

affinity nucleic acid ligands are generated from high-throughput in-vitro selection technology (SELEX) (Blind and Blank, 2015) making them a cheaper alternative to antibodies. They are the synthetic versions of bioreceptors with high binding strength, affinity and specificity, comparable, if not higher, than those of mAb (Savory et al., 2010). The dissociation constant (K_d) of PSA bound mAb were determined by direct ELISA method, reported at K_d of 0.2 – 164 nM (Corey et al., 1997). On the other hand, recent work by Park et. al (Park et al., 2016) demonstrated on an acoustofluidic separation method for screening of PSA-binding DNA aptamer, reported at K_d as low as 0.7 nM. However, the K_d of aptamers were also reported as high as 630 nM and 870 nM (estimated using Langmuir binding model) (Svobodova et al., 2013), depending on modification complexity of the ligands. Hence, selection of the aptamers-in-use plays major role in determination of their binding characteristics. On a different note, in several instances, aptamer also shown to have complement with the antibodies for generating high-performance analyses (Kim et al., 2010; Lakshmipriya et al., 2014).

4.1 PSA-Aptamer Functionalized Aptasensors

The desirability of aptamers binding properties are distinctive to its specific application. Typically, the favorable aptamer across full ranges of application is the one with fast association rate, slow dissociation rate, high affinity to the target molecules but discriminates the non-confirming molecules even at the slightest difference from the targets. Lower K_d results in higher binding strength toward the target biomolecules. Besides, as compared to mAb (MW ~150 kDa) (Janeway et al., 2001) with an approximately 10-12 nm in size (IgG-mAb) (Poghossian and Schöning, 2014) and 10-15 nm (IgE-mAb) (Maehashi et al., 2007), the aptamers are much smaller, at 6 – 40 kDa (Gopinath, 2011). Smaller molecules allow for protein-aptamer complexes to reside within the proximity of Debye screening length (~0.7-2.2 nm in bio-samples, i.e. blood, serum, and urine) (Elnathan et al., 2012) enabling low-fouling sensing mechanism of the bound complexes, hence improving detection sensitivity of the device (Maehashi and Matsumoto, 2009). Their size advantage was also reported to be favorable in enhancing the band structure changes in SWNT-FET channel or Schottky barrier contact upon the complex reactions (Kim et al., 2007). The binding affinity and specificity of aptamers can be improved by covalently linking them into a dimeric or multimeric ligand (using homodimerization process), however the homodimeric ligand moieties are susceptible to functional deficiency due to steric hindrance, or disheveled conformation of each module (Gopinath, 2011). Successful use of dual-ligand phage in electrochemical biosensor for sub-nanomolar detection of PCa antigen was demonstrated (Mohan et al., 2013). Though the team used the prostate-specific membrane antigen (PSMA), this method can also be implemented for an enhanced sensitivity and affinity detection of PSA in the future for bioelectronic detection. In a different work, Kavosi et al. (Kavosi et al., 2015) have reported on PSA-binding aptamer functionalized on the rGO-deposited GCE substrate. The highly selective PSA-binding aptamer sequence (5'-NH_2-(CH_2)6-ATTAAAGCTCGCCATCAAATAGC-3') was modified from the work

reported by Savory et al. (Savory et al., 2010) who applied genetic algorithm (GA) technique to post-SELEX screening for maturation of aptamers to enhance its affinity performance to PSA. The aptasensor, tested using the DPV measurement setup was reported to yield a linear detection to PSA concentrations ranging from 90 ng/ml down to 0.1 pg/ml, with LOD of 10 fg/ml (SNR = 3), which was at least two orders of magnitude higher than any antibody-functionalized, customized-electrodes devices-based immunosensors. Currently, one of the active teams working on a promising bioelectronics detection of PSA is P. Estrela and colleagues in University of Bath, as they are using DNA aptamer and high-performance detection has been achieved with the assistance of anti-fouling surface chemistry (Jolly et al., 2017, 2015). Another dynamic bioelectronics detection of PSA was demonstrated by Souada et al. (Souada et al., 2015) in this voltammetry analysis quinone-containing conducting copolymer has been used as a redox transducer. Further, combination of nanomaterials and aptamer are playing s central role in the development of aptasensors for the bioelectronics detection of PSA (Rahi et al., 2016; Yang et al., 2015). These achievements are due to the appealing superiorities of aptamers for their design flexibility and convenience for functional group modifications (Jayasena, 1999; Liu et al., 2009).

5. Future Visions

Nowadays, countless number of research works were reported on the PSA immunosensors which yield excellent linear detection ranges of antigen concentrations and LODs down to femto-values. However, these immunoassays are still lacking in the state-of-art features that would pave the route to commercialization. One of the prime challenges is to enable for detection in physiological conditions (i.e. in whole blood or serum). The overbearing sensitivity-limiting-factor from the Debye screening length must be mitigated to allow for immunosensing in high ionic strength solutions. One of the possible solutions was reported by Gao and the team (Gao et al., 2015) by incorporating a porous and biomolecule permeable polymer coating, FDA-approved biocompatible poly(ethylene glycol) (PEG) (Alconcel et al., 2011) onto the silicon nanowire field-effect transistors (SW-FETs) transducer. The technique was reported to allow for detection of PSA in the phosphate buffer (PB) with concentration up to 150 mM, compared to only ≤10 mM on the non-PEG modified SW-FETs sensor. Though, it is believed that PEG polymer increased the effective screening length adjacent to the sensing surface, however, the mechanism behind this phenomenon has not been fully comprehended. Further exploitation to understand this phenomenon may open up the revenues for future undertakings on the general designs of immunosensing devices. Other approaches include the application of smaller bioreceptors, such as antibody fragment (Fab) (Mustafaoglu et al., 2015), and aptamers (Heydari-Bafrooei and Shamszadeh, 2017; Jolly et al., 2017, 2015) to capture the PSA antigen. These reported techniques provide low-fouling immunosensing mechanism, improving the overall device performance as compared to the full-length monoclonal anti-PSA. However, extended studies on the performance of Fab and aptasensors' devices at the limit of physiological condition (i.e. ~0.7 nm in Debye screening length)

are crucial to elucidate their bottleneck point. Another reported sensitivity enhancement technique by (Zheng et al., 2010) reported the application of frequency domain measurement for immunobinding event was shown to improve the device sensitivity by 10-fold as compared to real-time measurement on the same device. Albeit the need for additional frequency domain measurement circuit, this technique is highly feasible for further development of high sensitivity biomolecular detection method. On the other hand, reversible binding of biomolecules allows for reusability of a biosensor. However, since the affinity reaction between the antigen-antibody complexes are almost irreversible (Gopinath et al., 2014), most of the currently reported immunoassays for detection of PSA are for single-use application. The research works on developing a reversible PSA immunosensors deserve more attention. The applications of cleavable chemical linkers are the most feasible technique that must be further studied, e.g. the reversible photocleavable crosslinking action on the photo-labile group (Stern et al., 2010), and the acid-labile cleavable linkers (Fan et al., 2016; Liu et al., 2008). These techniques reported on promising analytical binding recovery, as reported in relative standard deviation (RSD). Another important performance feature of a sensor device is the ability to preserve its native properties over an extended period of time. A study conducted by Ahn et al. (Ahn et al., 2012) has shown the prevalence of surface etching on the silicon dioxide (SiO_2) by the common buffers have led to erroneous sensing results. This is a vital factor that must be rectified in order to achieve the long-term stability of the developed sensing devices, especially the SiO_2-based devices, i.e. silicon NWs-FET, ambipolar conductor based devices on SOI substrate, and others that use SiO_2 for device passivation. One of the techniques reported in (Zhou et al., 2014) layered a thin film aluminum oxide (Al_2O_3) to passivate the silicon NWs-FET surface, resulting in a device with long-term stability of >4 months. Furthermore, layering with Al_2O_3/hafnium dioxide (HfO_2) extended its stability for >12 months. Though, these findings only reported on the silicon NWs-FET devices. Future studies on long-term stability improvement on other types of immunosensors are equally critical.

The current challenges in LoC system integration is noteworthy, and their resolution may hold the opportunity for the assays' success in clinical trials. The integration of microfluidic onto the biosensing system is an important aspect for developing a successful LoC system (Lafleur et al., 2016; Valencia et al., 2012), however, their exploitation in the prospect of PSA immunosensing is still in progression stage. In order to rectify the issue, many promising microfluidic architectures for pre-sensing manipulations can be adopted depending on pre-sensing requirements, such as pumpless liquids micromixer (Morrissette et al., 2017), proteins and cells separation system (Sarkar et al., 2016; Yousuff et al., 2017), also on-chip pre-concentration and labelling system (R. Yang et al., 2015). Besides, various integration techniques to ensure the conformance on the sensing devices have been reviewed (Temiz et al., 2015). On the other hand, the prevalence of current mobile era has excite the emergence of portable, smartphone-based quantitative detection of PSA (Barbosa et al., 2015). It is exciting to witness the future of wireless-based

immunodetection of PCa due to the readiness of semiconductors technology in the digital and radio frequency applications (Fathil et al., 2016b). Nevertheless, exploring the future visions on the sensing devices to enhance the performance using the ambipolar conduction mechanism and studies on the potentials of sensing the aberrant glycosylation of PSA serum as PCa marker will elevate the current state-of-art as detailed below.

5.1 Switching Polar Conduction (Unipolar vs. Ambipolar Devices)

Among all of electrochemical-based biosensors, FET-based devices offer the most interesting potentials for enhancing their field-effect characteristics to improve the sensing performances. In addition to low concentration, semi-quantitative results and compatible with standard metal oxide semiconductor process (easy integration to integrated circuit) (Adzhri et al., 2016; Fathil et al., 2016a, 2015), the conduction modes can be switched between unipolar and ambipolar conduction. As previously described, the unipolar (the holes or electrons are depending on the initial material properties or impurities added into the materials) and ambipolar (the holes or electrons carriers are controlled by the effect of additional gate biasing on the device substrate). **Table 1** shows the behavior of unipolar conduction for n- and p-type materials. The increase and decrease of the signal are depending on the transducer characteristics and biomolecule charges. Meanwhile, in ambipolar conduction, different device architectures, i.e. back-gate (Adzhri et al., 2017; Dai et al., 2013; Fernandes et al., 2012; Jang and Cho, 2015; Knopfmacher et al., 2010), double-gated (top- and bottom-gates or dual-sided gates) (Ahn et al., 2010; Koo et al., 2005), and triple-gated (combination of two-sided gates and back-gates) (Buitrago et al., 2014) have been demonstrated for various biomolecular detections. These device architectures can only be achieved in silicon-on-insulator wafer technology. With ambipolar conduction, the signal of detection can be improved with low concentration of detection. Their benefits have been demonstrated in various detections of biomolecule and can be extended to detect the serum PSA molecules. In a device with back-gate structure, the additional gate electrode can be patterned at the bottom or the side of the substrate (through the top silicon and buried oxide layer). Dai et al (Dai et al., 2013) demonstrated improved detection sensitivity of DNA and pH ranges exponentially in the sub-threshold regime. Fernandes et al (Fernandes et al., 2012) demonstrated the effects of back-gate biasing on the floating electrolytes in SOI-based nanoribbon. The electrolyte voltage is capacitively coupled to the applied back-gate bias, which resulting in a dual-gated sensor. The measurement setup shows lower threshold voltage and improved subthreshold slope. In a different work, Nernst limit of 60 mV/pH at room temperature has been demonstrated by Knopfmacher et al. (Knopfmacher et al., 2010). Double-gate nanowire FET as reported in (Ahn et al., 2010), the transducer area is located in between of two gates. Remarkable performance can be achieved in contrast to a single back-gate architecture. The gates allow for independent and precise voltage control to modulate the channel potential for detection of avian influenza virus. More complexed device has been demonstrated in (Buitrago et al., 2014) featuring a back-gate and two symmetrical side-gates with the presence of

the top 'liquid-gate'. The fabricated device (diameters of ~15-30 nm), was characterized in both dry and liquid environments (i.e. submerged in PBS of pH ~7.4). The team reported an improvement in overall electrostatic performance of the device, with steep sub-threshold slopes (SS) of < 75 mV/dec, low drain induced barrier lowering (DIBL) of < 20 mV/V and high transcoductance (gm > 10 μS). The device's demonstration in different pH solutions also showed changes in sensitivity proportional to the changes of pH values which induced the V_{th} shift as high as 200 mV/pH. Ambipolar conduction in FET-based devices therefore, provide remarkable pre-amplification performance of the electrical signal measured from the device transducer.

5.2 Aberrant Glycosylation of PSA for Detection of Prostate Cancer

Recent progressions in the fields of glycomics, genomics and proteomics have shed light onto other possible biomarkers for cancers prognosis values, and the detection of glycosylation of proteins may hold the answer (Belicky and Tkac, 2015). Glycosylation is the covalent attachment of carbohydrates moieties to proteins and lipids, and is one of the most vital post-translational modifications (PTMs) events in the human body. It is estimated more than half of proteins in the human body are glycosylated (Christiansen et al., 2014; Pihíková et al., 2015). The malignant transformation of healthy cells disrupts this glycosylation event, resulting in changes of glycan structure and glycosylation patterns. This glycan modification happens rapidly, predictably, and responsively towards the disease formation (Lebrilla and An, 2009), making the phenomenon a reliable biomarker for prediction of cancers. Therefore, aberrant glycosylated proteins have been associated to diseases due to tampered biological function and protein folding event. Meanwhile, the altered terminal glycan motifs on cell surface glycoproteins could provide prognosis value for cancers formation and metastatic behaviors (Christiansen et al., 2014).

Interestingly, all protein biomarkers available today are in glycosylated forms, including the PSA (Svarovsky and Joshi, 2014), albeit the current conventional method measures the PSA proteins abundance level. PSA has a single glycosylation site at Asn-45, and contains an approximately 8% attached N-glycans of sialylated complex biantennary carbohydrates, mostly in the form of core fucosylated (Okada et al., 2001; Peracaula et al., 2003). The presence of aberrantly fucosylated and sialylated structures, also, an increased branching in the suspected glycan proteins are principal markers for signs of PCa (Adamczyk et al., 2012). Llop et al. (Llop et al., 2016) have detected the decrease in core fucosylation and an increase in the α2,3-sialic acid percentage of PSA N-glycans in serum samples, which differentiated the high-risk PCa patients from the BPH and low-risk PCa patients. Though, the efficacy of PSA glycosylation detection by conventional glycomics analysis is limited by analysis speed and its throughput. There is no rapid system for large scale clinical analysis of human whole-serum glycoproteins, except for the only 'glycoblotting' technology which requires 14 hours to complete when combined with automated 'SweetBlot' system (Nishimura, 2011). Hence, this is where the roles of biosensors come into play. A research

team led by P. Estrela from University of Bath is among the emerging pioneers in the research and development of glycan – lectin based immunosensors for PCa. Recent work reported by Jolly et al. (Jolly et al., 2016) demonstrates an approach for dual quantification and multi-glycan profiling of fPSA by using DNA aptamer, realized by sandwich-type immunoreactions in chemiluminescence detection system. The assay, which was integrated onto the microfluidic platform, allows for parallel detection of fPSA abundance (using an aptamer – antibody sandwich assay), and the fPSA glycosylation levels (using the aptamer – lectin "S*ambucus nigra"* assay), with reported multiplexed detections within the relevant clinical range. The sandwich immunoassay demonstrated by Jolly et al. is a viable method for highly selective binding to an analyte from the complex serum. Though, the use EIS measurement setup would have allowed for a label-free detection technique, instead of using chemiluminescence label or tag which may hinder the binding sites of the sensing probe. The other shortcoming includes the need for sample preparation steps (i.e. pre-concentration and glycans-release procedures) (Svarovsky and Joshi, 2014) prior to detection which then can be solved by integration of sophisticated sample manipulation technique in microfluidic delivery system. However, the success of this method is subjected to future endeavor.

6. Conclusion

The field of bioelectronics converge the biological aspects to the electronics for the fine interpretation of biomolecular iterations. Electronic-mediated immunosensing using the FET device architecture enables for direct, fast, and real-time electrical detection of serum PSA marker with high sensitivity, selectivity, and in label-free manner. The silicon NWs-FET, specific peptide-based, and aptasensors for instance, offers the lowest LOD reported down to femto-range of detection. The size comparability and biocompatibility of both NWs and CNTs nanostructures to the biological molecules are the enabler toward the sensing performance down to single PSA molecular level. On the other hand, customized-electrodes devices-based biosensors provide as another option due to its portability, rapid, flexible and easier to mass produce with good sensitivity and reproducibility. The recent development works on SPEs have introduced interesting methods and applications ranging from printing materials improvement (Dossi et al., 2016; Jewell et al., 2016; Kamakoti et al., 2016), the magneto-controlled electrodes (Zhu et al., 2014), and the explore into feasibility of hand-drawn electrode (Bernalte et al., 2016). In short, customized-electrodes devices-based biosensors, developed on the SPEs and GCEs will pave the future path of biosensor's world, enabling the shift from in-lab PCa sensing devices into a portable LoC system with commercial values. Besides that, the authors also discussed on the future visions which include switching polar conduction (i.e. device-level implementation) and the sensing of aberrant glycosylated PSA using glycan – lectin sandwich assay (i.e. analyte/ligand detection method). We believe that further exploration into these aspects will realize the missions to convert the current

laborious PCa diagnosis methods into a PoC status for better portability, affordability and accessibility to all patients.

Acknowledgment

This work was supported by the Department of Higher Education, Ministry of Higher Education (MOHE) of Malaysia under the Fundamental Research Grant Scheme (FRGS), grant number 9003-00536.

References

Ablin, R.J., Soanes, W.A., Bronson, P., Witebsky, E., 1970. Precipitating antigens of the normal human prostate. J. Reprod. Fertil. 22, 573–574. doi:10.1530/jrf.0.0220573

Adamczyk, B., Tharmalingam, T., Rudd, P.M., 2012. Glycans as cancer biomarkers. Biochim. Biophys. Acta - Gen. Subj. 1820, 1347–1353. doi:10.1016/j.bbagen.2011.12.001

Adzhri, R., Md Arshad, M.K., Gopinath, S.C.B., Ruslinda, A.R., Fathil, M.F.M., Ayub, R.M., M. Nuzaihan, M.N., Voon, C.H., 2016. High-performance integrated field-effect transistor-based sensors. Anal. Chim. Acta 917, 1–18. doi:10.1016/j.aca.2016.02.042

Adzhri, R., Md Arshad, M.K., Gopinath, S.C.B., Ruslinda, A.R., Fathil, M.F.M., Ibau, C., M. Nuzaihan, M.N., 2017. Enhanced sensitivity mediated ambipolar conduction with p-type TiO_2 anatase transducer for biomarker capturing. Sensors Actuators A Phys. 259, 57–67. doi:10.1016/j.sna.2017.03.015

Ahn, J.H., Choi, S.J., Han, J.W., Park, T.J., Lee, S.Y., Choi, Y.K., 2010. Double-gate nanowire field-effect transistor for a biosensor. Nano Lett. 10, 2934–2938. doi:10.1021/nl1010965

Ahn, S., Spuhler, P.S., Chiari, M., Cabodi, M., Ünlü, M.S., 2012. Quantification of surface etching by common buffers and implications on the accuracy of label-free biological assays. Biosens. Bioelectron. 36, 222–229. doi:10.1016/j.bios.2012.04.020

Alconcel, S.N.S., Baas, A.S., Maynard, H.D., 2011. FDA-approved poly(ethylene glycol)–protein conjugate drugs. Polym. Chem. 2, 1442–1448. doi:10.1039/c1py00034a

Arduini, F., Ricci, F., Tuta, C.S., Moscone, D., Amine, A., Palleschi, G., 2006. Detection of carbamic and organophosphorous pesticides in water samples using a cholinesterase biosensor based on Prussian Blue-modified screen-printed electrode. Anal. Chim. Acta 580, 155–162. doi:10.1016/j.aca.2006.07.052

Arya, S.K., Bhansali, S., 2012. Anti-prostate specific antigen (anti-PSA) modified interdigitated microelectrode-based impedimetric biosensor for PSA detection. Biosens. J. 1, 1–7. doi:10.4303/BJ/H110601

Baade, P.D., Youlden, D.R., Cramb, S.M., Dunn, J., Gardiner, R. a, 2013. Epidemiology of prostate cancer in the Asia-Pacific region. Prostate Int. 1, 47–58. doi:10.12954/PI.12014

Barbosa, A.I., Gehlot, P., Sidapra, K., Edwards, A.D., Reis, N.M., 2015. Portable smartphone quantitation of prostate-specific antigen (PSA) in a fluoropolymer microfluidic device. Biosens. Bioelectron. 70, 5–14. doi:10.1016/j.bios.2015.03.006

Barton, A.C., Davis, F., Higson, S.P.J., 2008. Labeless immunosensor assay for prostate specific antigen with picogram per milliliter limits of detection based upon an ac impedance protocol. Anal. Chem. 80, 6198–6205. doi:10.1021/ac800491m

Belicky, S., Tkac, J., 2015. Can glycoprofiling be helpful in detecting prostate cancer? Chem. Pap. 69, 90–111. doi:10.1515/chempap-2015-0052

Berggren, C., Bjarnason, B., Johansson, G., 2001. Capacitive biosensors. Electroanalysis 13, 173–180. doi:10.1002/1521-4109(200103)13:3<173::AID-ELAN173>3.0.CO;2-B

Bergveld, P., 1991. A critical evaluation of direct electrical protein detection methods. Biosens. Bioelectron. 6, 55–72. doi:10.1016/0956-5663(91)85009-L

Bergveld, P., 1970. Development of an ion-sensitive solid-state device for neurophysiological measurements. IEEE Trans. Biomed. Eng. BME-17, 70–71. doi:10.1109/TBME.1970.4502688

Bernalte, E., Foster, C.W., Brownson, D.A.C., Mosna, M., Smith, G.C., Banks, C.E., 2016. Pencil it in: Exploring the feasibility of hand-drawn pencil electrochemical sensors and their direct

comparison to screen-printed electrodes. Biosensors 6, 45. doi:10.3390/bios6030045

Bernalte, E., Sánchez, C.M., Gil, E.P., 2011. Determination of mercury in ambient water samples by anodic stripping voltammetry on screen-printed gold electrodes. Anal. Chim. Acta 689, 60–64. doi:10.1016/j.aca.2011.01.042

Bienz, M., Saad, F., 2015. Androgen-deprivation therapy and bone loss in prostate cancer patients: A clinical review. Bonekey Rep. 4, 716. doi:10.1038/bonekey.2015.85

Blind, M., Blank, M., 2015. Aptamer selection technology and recent advances. Mol. Ther. - Nucleic Acids 4, e223. doi:10.1038/mtna.2014.74

Brawer, M.K., Chetner, M.P., Beatie, J., Buchner, D.M., Vessella, R.L., Lange, P.H., 1992. Screening for prostatic carcinoma with prostate specific antigen. J. Urol. 147, 841–845.

Buitrago, E., Badia, M.F.B., Georgiev, Y.M., Yu, R., Lotty, O., Holmes, J.D., Nightingale, A.M., Guerin, H.M., Ionescu, A.M., 2014. Electrical characterization of high performance, liquid gated vertically stacked SiNW-based 3D FET biosensors. Sensors Actuators B Chem. 199, 291–300. doi:10.1016/j.snb.2014.03.099

Catalona, W.J., Bartsch, G., Rittenhouse, H.G., Evans, C.L., Linton, H.J., Amirkhan, A., Horninger, W., Klocker, H., Mikolajczyk, S.D., 2003. Serum pro prostate-specific antigen improves cancer detection compared to free and complexed prostate-specific antigen in men With prostate-specific antigen 2 to 4 ng/ml. J. Urol. 170, 2181–2185. doi:10.1097/01.ju.0000095460.12999.43

Catalona, W.J., Smith, D.S., Ratliff, T.L., Basler, J.W., 1993. Detection of organ-confined prostate cancer is increased through prostate-specific antigen—based screening. JAMA J. Am. Med. Assoc. 270, 948–954. doi:10.1001/jama.1993.03510080052031

Catalona, W.J., Smith, D.S., Wolfert, R.L., Wang, T.J., Rittenhouse, H.G., Ratliff, T.L., Nadler, R.B., 1995. Evaluation of percentage of free serum prostate-specific antigen to improve specificity of prostate cancer screening. JAMA J. Am. Med. Assoc. 274, 1214–1220. doi:10.1001/jama.274.15.1214

Chen, K.I., Li, B.R., Chen, Y.T., 2011. Silicon nanowire field-effect transistor-based biosensors for biomedical diagnosis and cellular recording investigation. Nano Today 6, 131–154. doi:10.1016/j.nantod.2011.02.001

Cheng, S., Hotani, K., Hideshima, S., Kuroiwa, S., Nakanishi, T., Hashimoto, M., Mori, Y., Osaka, T., 2014. Field Effect Transistor Biosensor Using Antigen Binding Fragment for Detecting Tumor Marker in Human Serum. Materials (Basel). 7, 2490–2500. doi:10.3390/ma7042490

Chikkaveeraiah, B. V., Bhirde, A., Malhotra, R., Patel, V., Gutkind, J.S., Rusling, J.F., 2009. Single-Wall Carbon Nanotube Forest Arrays for Immunoelectrochemical Measurement of Four Protein Biomarkers for Prostate Cancer. Anal. Chem. 81, 9129–9134. doi:10.1021/ac9018022

Choi, J.H., Kim, H.S., Choi, J.W., Hong, J.W., Kim, Y.K., Oh, B.K., 2013. A novel Au-nanoparticle biosensor for the rapid and simple detection of PSA using a sequence-specific peptide cleavage reaction. Biosens. Bioelectron. 49, 415–419. doi:10.1016/j.bios.2013.05.042

Chornokur, G., Arya, S.K., Phelan, C., Tanner, R., Bhansali, S., 2011. Impedance-based miniaturized biosensor for ultrasensitive and fast prostate-specific antigen detection. J. Sensors 2011, 1–7. doi:10.1155/2011/983752

Christiansen, M.N., Chik, J., Lee, L., Anugraham, M., Abrahams, J.L., Packer, N.H., 2014. Cell surface protein glycosylation in cancer. Proteomics 14, 525–546. doi:10.1002/pmic.201300387

Citartan, M., Gopinath, S.C.B., Tominaga, J., Tan, S.-C., Tang, T.-H., 2012. Assays for aptamer-based platforms. Biosens. Bioelectron. 34, 1–11. doi:10.1016/j.bios.2012.01.002

Coleman, R.E., 2001. Metastatic bone disease: clinical features, pathophysiology and treatment strategies. Cancer Treat. Rev. 27, 165–176. doi:10.1053/ctrv.2000.0210

Corey, E., Wegner, S.K., Stray, J.E., Corey, M.J., Arfman, E.W., Lange, P.H., Vessella, R.L., 1997. Characterization of 10 new monoclonal antibodies against prostate-specific antigen by analysis of affinity, specificity and function in sandwich assays. Int. J. Cancer 71, 1019–1028. doi:10.1002/(SICI)1097-0215(19970611)71:6<1019::AID-IJC18>3.0.CO;2-8

Crawford, E.D., DeAntoni, E.P., Etzioni, R., Schaefer, V.C., Olson, R.M., ROSS, C.A., 1996. Serum prostate-specific antigen and digital rectal examination for early detection of prostate cancer in a national community-based program. Urology 47, 863–869. doi:10.1016/S0090-4295(96)00061-1

Dai, P., Gao, A., Lu, N., Li, T., Wang, Y., 2013. A back-gate controlled silicon nanowire sensor with sensitivity improvement for DNA and pH detection. Jpn. J. Appl. Phys. 52, 121301. doi:10.7567/JJAP.52.121301

Davis, F., Higson, S.P.J., 2010. Label-free immunochemistry approach to detect and identity antibiotics in milk. Pediatr. Res. 67, 476–480. doi:10.1203/PDR.0b013e3181d61c0c

Denmeade, S.R., Isaacs, J.T., 2002. A history of prostate cancer treatment. Nat. Rev. Cancer 2, 389–396. doi:10.1038/nrc801

Ding, L., You, J., Kong, R., Qu, F., 2013. Signal amplification strategy for sensitive immunoassay of prostate specific antigen (PSA) based on ferrocene incorporated polystyrene spheres. Anal. Chim. Acta 793, 19–25. doi:10.1016/j.aca.2013.07.054

Dossi, C., Monticelli, D., Pozzi, A., Recchia, S., 2016. Exploiting chemistry to improve performance of screen-printed, bismuth film electrodes (SP-BiFE). Biosensors 6, 38. doi:10.3390/bios6030038

Elnathan, R., Kwiat, M., Pevzner, A., Engel, Y., Burstein, L., Khatchtourints, A., Lichtenstein, A., Kantaev, R., Patolsky, F., 2012. Biorecognition layer engineering: Overcoming screening limitations of nanowire-based FET devices. Nano Lett. 12, 5245–5254. doi:10.1021/nl302434w

Escamilla-Gomez, V., Hernandez-Santos, D., Gonzalez-Garcia, M.B., Pingarron-Carrazon, J.M., Costa-Garcia, A., 2009. Simultaneous detection of free and total prostate specific antigen on a screen-printed electrochemical dual sensor. Biosens. Bioelectron. 24, 2678–2683. doi:10.1016/j.bios.2009.01.043

Estévez, M.C., Huang, Y.-F., Kang, H., O'Donoghue, M.B., Bamrungsap, S., Yan, J., Chen, X., Tan, W., 2010. Nanoparticle–aptamer conjugates for cancer cell targeting and detection, in: Grobmyer, S.R., Moudgil, B.M. (Eds.), Cancer Nanotechnology: Methods and Protocols (Methods in Molecular Biology). Humana Press, New York, pp. 235–248. doi:10.1007/978-1-60761-609-2_16

Etzioni, R., Penson, D.F., Legler, J.M., di Tommaso, D., Boer, R., Gann, P.H., Feuer, E.J., 2002. Overdiagnosis due to prostate-specific antigen screening: Lessons from U.S. prostate cancer incidence trends. J. Natl. Cancer Inst. 94, 981–90. doi:10.1093/jnci/94.13.981

Fan, D., Li, N., Ma, H., Li, Y., Hu, L., Du, B., Wei, Q., 2016. Electrochemical immunosensor for detection of prostate specific antigen based on an acid cleavable linker into MSN-based controlled release system. Biosens. Bioelectron. 85, 580–586. doi:10.1016/j.bios.2016.05.063

Fathil, M.F.M., Md Arshad, M.K., Gopinath, S.C.B., Hashim, U., Adzhri, R., Ayub, R.M., Ruslinda, A.R., M. Nuzaihan, M.N., Azman, A.H., Zaki, M., Tang, T.H., 2015. Diagnostics on acute myocardial infarction: Cardiac troponin biomarkers. Biosens. Bioelectron. 70, 209–220. doi:10.1016/j.bios.2015.03.037

Fathil, M.F.M., Md Arshad, M.K., Ruslinda, A.R., Gopinath, S.C.B., M. Nuzaihan, M.N., Adzhri, R., Hashim, U., Lam, H.Y., 2016a. Substrate-gate coupling in ZnO-FET biosensor for cardiac troponin I detection. Sensors Actuators B Chem. 242, 1142–1154. doi:10.1016/j.snb.2016.09.131

Fathil, M.F.M., Md Arshad, M.K., Ruslinda, A.R., M. Nuzaihan, M.N., Gopinath, S.C.B., Adzhri, R.,

Hashim, U., 2016b. Progression in sensing cardiac troponin biomarker charge transductions on semiconducting nanomaterials. Anal. Chim. Acta 935, 30–43. doi:10.1016/j.aca.2016.06.012

Ferlay, J., Shin, H.R., Bray, F., Forman, D., Mathers, C., Parkin, D.M., 2010. Estimates of worldwide burden of cancer in 2008: GLOBOCAN 2008. Int. J. Cancer 127, 2893–2917. doi:10.1002/ijc.25516

Fernandes, P.G., Chapman, R.A., Seitz, O., Stiegler, H.J., Wen, H.C., Chabal, Y.J., Vogel, E.M., 2012. Effect of back-gate biasing on floating electrolytes in silicon-on-insulator-based nanoribbon sensors. IEEE Electron Device Lett. 33, 447–449. doi:10.1109/LED.2011.2179115

Gao, N., Zhou, W., Jiang, X., Hong, G., Fu, T.M., Lieber, C.M., 2015. General strategy for biodetection in high ionic strength solutions using transistor-based nanoelectronic sensors. Nano Lett. 15, 2143–8. doi:10.1021/acs.nanolett.5b00133

Gopinath, S.C.B., 2011. Aptamers, in: Encyclopedia of Analytical Chemistry. John Wiley & Sons, Ltd, Chichester, UK, pp. 1–29. doi:10.1002/9780470027318.a1402.pub2

Gopinath, S.C.B., Tang, T.H., Citartan, M., Chen, Y., Lakshmipriya, T., 2014. Current aspects in immunosensors. Biosens. Bioelectron. 57, 292–302. doi:10.1016/j.bios.2014.02.029

Guan, J.G., Miao, Y.Q., Zhang, Q.J., 2004. Impedimetric biosensors. J. Biosci. Bioeng. 97, 219–226. doi:10.1263/jbb.97.219

Hankey, B.F., Feuer, E.J., Clegg, L.X., Hayes, R.B., Legler, J.M., Prorok, P.C., Ries, L. a, Merrill, R.M., Kaplan, R.S.K., 1999. Cancer surveillance series: Interpreting trends in prostate cancer part I: Evidence of the effects of screening in recent prostate cancer incidence, mortality, and survival rates. JNCI J. Natl. Cancer Inst. 91, 1017–1024. doi:10.1093/jnci/91.12.1017

Härmä, H., Pelkkikangas, A.M., Soukka, T., Huhtinen, P., Huopalahti, S., Lövgren, T., 2003. Sensitive miniature single-particle immunoassay of prostate-specific antigen using time-resolved fluorescence. Anal. Chim. Acta 482, 157–164. doi:10.1016/S0003-2670(03)00207-1

Heydari-Bafrooei, E., Shamszadeh, N.S., 2017. Electrochemical bioassay development for ultrasensitive aptasensing of prostate specific antigen. Biosens. Bioelectron. 91, 284–292. doi:10.1016/j.bios.2016.12.048

Hsiao, C.Y., Lin, C.H., Hung, C.H., Su, C.J., Lo, Y.R., Lee, C.C., Lin, H.C., Ko, F.H., Huang, T.Y., Yang, Y.S., 2009. Novel poly-silicon nanowire field effect transistor for biosensing application. Biosens. Bioelectron. 24, 1223–1229. doi:10.1016/j.bios.2008.07.032

Huang, W., Diallo, A.K., Dailey, J.L., Besar, K., Katz, H.E., 2015. Electrochemical processes and mechanistic aspects of field-effect sensors for biomolecules. J. Mater. Chem. C 3, 6445–6470. doi:10.1039/C5TC00755K

Huang, Y., Wang, T.H., Jiang, J.H., Shen, G.L., Yu, R.Q., 2009. Prostate-specific antigen detection using microgapped electrode array immunosensor with enzymatic silver deposition. Clin. Chem. 55, 964–971. doi:10.1373/clinchem.2008.116582

Huang, Y.W., Wu, C.S., Chuang, C.K., Pang, S.T., Pan, T.M., Yang, Y.S., Ko, F.H., 2013. Real-time and label-free detection of the prostate-specific antigen in human serum by a polycrystalline silicon nanowire field-effect transistor biosensor. Anal. Chem. 85, 7912–7918. doi:10.1021/ac401610s

Hummers, W.S., Offeman, R.E., 1958. Preparation of graphitic oxide. J. Am. Chem. Soc. 80, 1339–1339. doi:10.1021/ja01539a017

Ito, K., 2014. Prostate cancer in Asian men. Nat. Rev. Urol. 11, 197–212. doi:10.1038/nrurol.2014.42

Ito, K., Nishimura, W., Maeda, M., Gomi, K., Inouye, S., Arakawa, H., 2007. Highly sensitive and rapid tandem bioluminescent immunoassay using aequorin labeled Fab fragment and

biotinylated firefly luciferase. Anal. Chim. Acta 588, 245–251. doi:10.1016/j.aca.2007.02.005

Janeway, C.A., Travers, P., Walport, M., Shlomchik, M., 2001. The recognition of antigen, in: Austin, P., Lawrence, E. (Eds.), Immunobiology: The Immune System in Health and Disease. Garland Publishing, New York, p. 117.

Jang, H.J., Cho, W.J., 2015. Performance enhancement of capacitive-coupling dual-gate ion-sensitive field-effect transistor in ultra-thin-body. Sci. Rep. 4, 5284. doi:10.1038/srep05284

Jayasena, S.D., 1999. Aptamers: An emerging class of molecules that rival antibodies in diagnostics. Clin. Chem. 45, 1628–1650. doi:10.1038/mtna.2014.74

Jewell, E., Philip, B., Greenwood, P., 2016. Improved manufacturing performance of screen-printed carbon electrodes through material formulation. Biosensors 6, 30. doi:10.3390/bios6030030

Jolly, P., Damborsky, P., Madaboosi, N., Soares, R.R.G., Chu, V., Conde, J.P., Katrlik, J., Estrela, P., 2016. DNA aptamer-based sandwich microfluidic assays for dual quantification and multi-glycan profiling of cancer biomarkers. Biosens. Bioelectron. 79, 313–319. doi:10.1016/j.bios.2015.12.058

Jolly, P., Formisano, N., Tkáč, J., Kasák, P., Frost, C.G., Estrela, P., 2015. Label-free impedimetric aptasensor with antifouling surface chemistry: A prostate-specific antigen case study. Sensors Actuators B Chem. 209, 306–312. doi:10.1016/j.snb.2014.11.083

Jolly, P., Zhurauski, P., Hammond, J.L., Miodek, A., Liébana, S., Bertok, T., Tkáč, J., Estrela, P., 2017. Self-assembled gold nanoparticles for impedimetric and amperometric detection of a prostate cancer biomarker. Sensors Actuators B Chem. 251, 637–643. doi:10.1016/j.snb.2017.05.040

Kalantar-zadeh, K., Ou, J.Z., 2016. Biosensors based on two-dimensional MoS_2 . ACS Sensors 1, 5–16. doi:10.1021/acssensors.5b00142

Kamakoti, V., Selvam, A.P., Shanmugam, N.R., Muthukumar, S., Prasad, S., 2016. Flexible molybdenum electrodes towards designing affinity based protein biosensors. Biosensors 6, 36. doi:10.3390/bios6030036

Kavosi, B., Salimi, A., Hallaj, R., Moradi, F., 2015. Ultrasensitive electrochemical immunosensor for PSA biomarker detection in prostate cancer cells using gold nanoparticles/PAMAM dendrimer loaded with enzyme linked aptamer as integrated triple signal amplification strategy. Biosens. Bioelectron. 74, 915–923. doi:10.1016/j.bios.2015.07.064

Kim, J.P., Lee, B.Y., Lee, J., Hong, S., Sim, S.J., 2009. Enhancement of sensitivity and specificity by surface modification of carbon nanotubes in diagnosis of prostate cancer based on carbon nanotube field effect transistors. Biosens. Bioelectron. 24, 3372–3378. doi:10.1016/j.bios.2009.04.048

Kim, S., Lee, J., Lee, S.J., Lee, H.J., 2010. Ultra-sensitive detection of IgE using biofunctionalized nanoparticle-enhanced SPR. Talanta 81, 1755–1759. doi:10.1016/j.talanta.2010.03.036

Kim, S.N., Rusling, J.F., Papadimitrakopoulos, F., 2007. Carbon nanotubes for electronic and electrochemical detection of biomolecules. Adv. Mater. 19, 3214–3228. doi:10.1002/adma.200700665

Knopfmacher, O., Tarasov, A., Fu, W., Wipf, M., Niesen, B., Calame, M., Schönenberger, C., 2010. Nernst limit in dual-gated Si-nanowire FET sensors. Nano Lett. 10, 2268–2274. doi:10.1021/nl100892y

Koo, S.M., Li, Q., Edelstein, M.D., Richter, C.A., Vogel, E.M., 2005. Enhanced channel modulation in dual-gated silicon nanowire transistors. Nano Lett. 5, 2519–2523. doi:10.1021/nl051855i

Kovtyukhova, N.I., Ollivier, P.J., Martin, B.R., Mallouk, T.E., Chizhik, S.A., Buzaneva, E. V, Gorchinskiy, A.D., 1999. Layer-by-layer assembly of ultrathin composite films from micron-sized graphite oxide sheets and polycations. Chem. Mater. 11, 771–778. doi:10.1021/cm981085u

Kumar, J., D'Souza, S.F., 2011. Microbial biosensor for detection of methyl parathion using screen printed carbon electrode and cyclic voltammetry. Biosens. Bioelectron. 26, 4289–4293. doi:10.1016/j.bios.2011.04.027

Lafleur, J.P., Jönsson, A., Senkbeil, S., Kutter, J.P., 2016. Recent advances in lab-on-a-chip for biosensing applications. Biosens. Bioelectron. 76, 213–233. doi:10.1016/j.bios.2015.08.003

Lakshmipriya, T., Horiguchi, Y., Nagasaki, Y., 2014. Co-immobilized poly(ethylene glycol)-block-polyamines promote sensitivity and restrict biofouling on gold sensor surface for detecting factor IX in human plasma. Analyst 139, 3977. doi:10.1039/C4AN00168K

Le Floch, F., Ho, H.A., Harding-Lepage, P., Bédard, M., Neagu-Plesu, R., Leclerc, M., 2005. Ferrocene-functionalized cationic polythiophene for the label-free electrochemical detection of DNA. Adv. Mater. 17, 1251–1254. doi:10.1002/adma.200401474

Lebrilla, C.B., An, H.J., 2009. The prospects of glycan biomarkers for the diagnosis of diseases. Mol. BioSyst. 5, 17–20. doi:10.1039/B811781K

Lee, J., Dak, P., Lee, Y., Park, H., Choi, W., Alam, M.A., Kim, S., 2014. Two-dimensional layered MoS_2 biosensors enable highly sensitive detection of biomolecules. Sci. Rep. 4, 7352. doi:10.1038/srep07352

Li, C., Curreli, M., Lin, H., Lei, B., Ishikawa, F.N., Datar, R., Cote, R.J., Thompson, M.E., Zhou, C., 2005. Complementary detection of prostate-specific antigen using In_2O_3 nanowires and carbon nanotubes. J. Am. Chem. Soc. 127, 12484–12485. doi:10.1021/ja053761g

Li, X., Li, W., Yang, Q., Gong, X., Guo, W., Dong, C., Liu, J., Xuan, L., Chang, J., 2014. Rapid and quantitative detection of prostate-specific antigen with a quantum dot nanobeads-based immunochromatography test strip. ACS Appl Mater Interfaces 6, 6406–6414. doi:10.1021/am5012782

Lin, C.H., Hung, C.H., Hsiao, C.Y., Lin, H.C., Ko, F.H., Yang, Y.S., 2009. Poly-silicon nanowire field-effect transistor for ultrasensitive and label-free detection of pathogenic avian influenza DNA. Biosens. Bioelectron. 24, 3019–3024. doi:10.1016/j.bios.2009.03.014

Lin, C.Y., Vasantha, V.S., Ho, K.C., 2009. Detection of nitrite using poly(3,4-ethylenedioxythiophene) modified SPCEs. Sensors Actuators B Chem. 140, 51–57. doi:10.1016/j.snb.2009.04.047

Lin, Y.Y., Wang, J., Liu, G., Wu, H., Wai, C.M., Lin, Y., 2008. A nanoparticle label/immunochromatographic electrochemical biosensor for rapid and sensitive detection of prostate-specific antigen. Biosens. Bioelectron. 23, 1659–1665. doi:10.1016/j.bios.2008.01.037

Lisdat, F., Schäfer, D., 2008. The use of electrochemical impedance spectroscopy for biosensing. Anal. Bioanal. Chem. 391, 1555–1567. doi:10.1007/s00216-008-1970-7

Liu, J., Cao, Z., Lu, Y., 2009. Functional nucleic acid sensors. Chem. Rev. 109, 1948–1998. doi:10.1021/cr030183i

Liu, K.K., Zhang, W., Lee, Y.H., Lin, Y.C., Chang, M.T., Su, C.Y., Chang, C.S., Li, H., Shi, Y., Zhang, H., Lai, C.S., Li, L.J., 2012. Growth of large-area and highly crystalline MoS_2 thin layers on insulating substrates. Nano Lett. 12, 1538–1544. doi:10.1021/nl2043612

Liu, S., Zhang, X., Wu, Y., Tu, Y., He, L., 2008. Prostate-specific antigen detection by using a reusable amperometric immunosensor based on reversible binding and leasing of HRP-anti-PSA from phenylboronic acid modified electrode. Clin. Chim. Acta 395, 51–56. doi:10.1016/j.cca.2008.04.031

Llop, E., Ferrer-Batallé, M., Barrabés, S., Guerrero, P.E., Ramírez, M., Saldova, R., Rudd, P.M., Aleixandre, R.N., Comet, J., de Llorens, R., Peracaula, R., 2016. Improvement of prostate cancer diagnosis by detecting PSA glycosylation-specific changes. Theranostics 6, 1190–1204. doi:10.7150/thno.15226

M. Nuzaihan, M.N., Hashim, U., Md Arshad, M.K., Kasjoo, S.R., Rahman, S.F.A., Ruslinda, A.R., Fathil, M.F.M., Adzhri, R., Shahimin, M.M., 2016. Electrical detection of dengue virus (DENV) DNA oligomer using silicon nanowire biosensor with novel molecular gate control. Biosens. Bioelectron. 83, 106–114. doi:10.1016/j.bios.2016.04.033

Maehashi, K., Katsura, T., Kerman, K., Takamura, Y., Matsumoto, K., Tamiya, E., 2007. Label-free protein biosensor based on aptamer-modified carbon nanotube field-effect transistors. Anal. Chem. 79, 782–787. doi:10.1021/ac060830g

Maehashi, K., Matsumoto, K., 2009. Label-free electrical detection using carbon nanotube-based biosensors. Sensors 9, 5368–5378. doi:10.3390/s90705368

Mak, K.F., Lee, C., Hone, J., Shan, J., Heinz, T.F., 2010. Atomically thin MoS_2 : A new direct-gap semiconductor. Phys. Rev. Lett. 105, 136805. doi:10.1103/PhysRevLett.105.136805

Malvano, F., Albanese, D., Crescitelli, A., Pilloton, R., Esposito, E., 2016. Impedimetric label-free immunosensor on disposable modified screen-printed electrodes for Ochratoxin A. Biosensors 6, 33. doi:10.3390/bios6030033

Masereel, B., Dinguizli, M., Bouzin, C., Moniotte, N., Feron, O., Gallez, B., Vander Borght, T., Michiels, C., Lucas, S., 2011. Antibody immobilization on gold nanoparticles coated layer-by-layer with polyelectrolytes. J. Nanoparticle Res. 13, 1573–1580. doi:10.1007/s11051-010-9908-3

Matsumoto, K., Konishi, N., Hiasa, Y., Kimura, E., Takahashi, Y., Shinohara, K., Samori, T., 1999. A highly sensitive enzyme-linked immunoassay for serum free prostate specific antigen (f-PSA). Clin. Chim. Acta 281, 57–69. doi:10.1016/S0009-8981(98)00208-3

Matsumoto, K., Konishi, N., Samori, T., Kimura, E., Doi, M., Kato, S., Yuki, Y. ichi, 2000. ELISA for a complexed antigen with a monoclonal antibody blocking reaction with the free antigen—assay-specific for complexed prostate-specific antigen. J. Immunol. Methods 234, 99–106. doi:10.1016/S0022-1759(99)00209-4

Mbarek, H., Saadoun, M., Bessaïs, B., 2007. Porous screen printed indium tin oxide (ITO) for NOx gas sensing. Phys. status solidi 4, 1903–1907. doi:10.1002/pssc.200674315

McAllister, M.J., Li, J.L., Adamson, D.H., Schniepp, H.C., Abdala, A.A., Liu, J., Herrera-Alonso, M., Milius, D.L., Car, R., Prud'homme, R.K., Aksay, I.A., 2007. Single sheet functionalized graphene by oxidation and thermal expansion of graphite. Chem. Mater. 19, 4396–4404. doi:10.1021/cm0630800

Mettlin, C., Murphy, G.P., Lee, F., Littrup, P.J., Chesley, A., Babaian, R., Badalament, R., Kane, R.A., Mostofi, F.K., 1993. Characteristics of prostate cancers detected in a multimodality early detection program. The Investigators of the American Cancer Society-National Prostate Cancer Detection Project. Cancer 72, 1701–1708.

Metzler-Nolte, N., Salmain, M., 2008. The Bioorganometallic Chemistry of Ferrocene, in: Ferrocenes. John Wiley & Sons, Ltd, Chichester, UK, pp. 499–639. doi:10.1002/9780470985663.ch13

Mikolajczyk, S.D., Catalona, W.J., Evans, C.L., Linton, H.J., Millar, L.S., Marker, K.M., Katir, D., Amirkhan, A., Rittenhouse, H.G., 2004. Proenzyme forms of prostate-specific antigen in serum improve the detection of prostate cancer. Clin. Chem. 50, 1017–1025. doi:10.1373/clinchem.2003.026823

Mohan, K., Donavan, K.C., Arter, J.A., Penner, R.M., Weiss, G.A., 2013. Sub-nanomolar detection of prostate-specific membrane antigen in synthetic urine by synergistic, dual-ligand phage. J. Am. Chem. Soc. 135, 7761–7767. doi:10.1021/ja4028082

Morata, A., Viricelle, J.P., Tarancon, A., Dezanneau, G., Pijolat, C., Peiro, F., Morante, J.R., 2007. Development and characterisation of a screen-printed mixed potential gas sensor. Sensors Actuators B Chem. 130, 561–566. doi:10.1016/j.snb.2007.09.086

Morrissette, J.M., Mahapatra, P.S., Ghosh, A., Ganguly, R., Megaridis, C.M., 2017. Rapid, self-driven liquid mixing on open-surface microfluidic platforms. Sci. Rep. 7, 1800. doi:10.1038/s41598-017-01725-0

Murphy, L., Watson, R.W., 2012. Patented prostate cancer biomarkers. Nat. Rev. Urol. 9, 464–472. doi:10.1038/nrurol.2012.130

Mustafaoglu, N., Alves, N.J., Bilgicer, B., 2015. Oriented immobilization of Fab fragments by site-specific biotinylation at the conserved nucleotide binding site for enhanced antigen detection. Langmuir 31, 9728–9736. doi:10.1021/acs.langmuir.5b01734

Naylor, C.H., Kybert, N.J., Schneier, C., Xi, J., Romero, G., Saven, J.G., Liu, R., Johnson, A.T.C., 2016. Scalable production of molybdenum disulfide based biosensors. ACS Nano 10, 6173–6179. doi:10.1021/acsnano.6b02137

Ndiaye, A.L., Delile, S., Brunet, J., Varenne, C., Pauly, A., 2016. Electrochemical sensors based on screen-printed electrodes: The use of phthalocyanine derivatives for application in VFA detection. Biosensors 6, 46. doi:10.3390/bios6030046

Nishimura, S.I., 2011. Toward automated glycan analysis, in: Advances in Carbohydrate Chemistry and Biochemistry. Elsevier Inc., pp. 219–271. doi:10.1016/B978-0-12-385520-6.00005-4

Nurmikko, P., Pettersson, K., Piironen, T., Hugosson, J., Lilja, H., 2001. Discrimination of prostate cancer from benign disease by plasma measurement of intact, free prostate-specific antigen lacking an internal cleavage site at Lys145-Lys146. Clin. Chem. 47, 1415–23.

Okada, T., Sato, Y., Kobayashi, N., Sumida, K., Satomura, S., Matsuura, S., Takasaki, M., Endo, T., 2001. Structural characteristics of the N-glycans of two isoforms of prostate-specific antigens purified from human seminal fluid. Biochim. Biophys. Acta - Gen. Subj. 1525, 149–160. doi:10.1016/S0304-4165(00)00182-3

Okuno, J., Maehashi, K., Kerman, K., Takamura, Y., Matsumoto, K., Tamiya, E., 2007. Label-free immunosensor for prostate-specific antigen based on single-walled carbon nanotube array-modified microelectrodes. Biosens. Bioelectron. 22, 2377–2381. doi:10.1016/j.bios.2006.09.038

Otero, T.F., Martinez, J.G., Hosaka, K., Okuzaki, H., 2011. Electrochemical characterization of PEDOT–PSS–Sorbitol electrodes. Sorbitol changes cation to anion interchange during reactions. J. Electroanal. Chem. 657, 23–27. doi:10.1016/j.jelechem.2011.02.017

Paine, A.J., 1990. Dispersion polymerization of styrene in polar solvents. 7. A simple mechanistic model to predict particle size. Macromolecules 23, 3109–3117. doi:10.1021/ma00214a013

Park, J.W., Lee, S.J., Ren, S., Lee, S., Kim, S., Laurell, T., 2016. Acousto-microfluidics for screening of ssDNA aptamer. Sci. Rep. 6, 27121. doi:10.1038/srep27121

Patolsky, F., Timko, B.P., Zheng, G., Lieber, C.M., 2007. Nanowire-based nanoelectronic devices in the life sciences. MRS Bull. 32, 142–149. doi:10.1557/mrs2007.47

Pentyala, S., Whyard, T., Pentyala, S., Muller, J., Pfail, J., Parmar, S., Helguero, C., Khan, S., 2016. Prostate cancer markers: An update (Review). Biomed. Reports 4, 263–268. doi:10.3892/br.2016.586

Peracaula, R., Tabarés, G., Royle, L., Harvey, D.J., Dwek, R.A., Rudd, P.M., de Llorens, R., 2003. Altered glycosylation pattern allows the distinction between prostate-specific antigen (PSA) from normal and tumor origins. Glycobiology 13, 457–70. doi:10.1093/glycob/cwg041

Pihíková, D., Kasák, P., Tkac, J., 2015. Glycoprofiling of cancer biomarkers: Label-free electrochemical lectin-based biosensors. Open Chem. 13, 636–655. doi:10.1515/chem-2015-0082

Poghossian, A., Schöning, M.J., 2014. Label-free sensing of biomolecules with field-effect devices for clinical applications. Electroanalysis 26, 1197–1213. doi:10.1002/elan.201400073

Presnova, G., Presnov, D., Krupenin, V., Grigorenko, V., Trifonov, A., Andreeva, I., Ignatenko, O., Egorov, A., Rubtsova, M., 2017. Biosensor based on a silicon nanowire field-effect transistor functionalized by gold nanoparticles for the highly sensitive determination of prostate-specific antigen. Biosens. Bioelectron. 88, 283–289. doi:10.1016/j.bios.2016.08.054

Rahi, A., Sattarahmady, N., Heli, H., 2016. Label-free electrochemical aptasensing of the human prostate-specific antigen using gold nanospears. Talanta 156–157, 218–224. doi:10.1016/j.talanta.2016.05.029

Rahman, M.A., Son, J.I., Won, M.S., Shim, Y.B., 2009. Gold nanoparticles doped conducting polymer nanorod electrodes: Ferrocene catalyzed aptamer-based thrombin immunosensor. Anal. Chem. 81, 6604–11. doi:10.1021/ac900285v

Rigau, M., Ortega, I., Mir, M.C., Ballesteros, C., Garcia, M., Llauradó, M., Colás, E., Pedrola, N., Montes, M., Sequeiros, T., Ertekin, T., Majem, B., Planas, J., Ruiz, A., Abal, M., Sánchez, A., Morote, J., Reventós, J., Doll, A., 2011. A three-gene panel on urine increases PSA specificity in the detection of prostate cancer. Prostate 71, 1736–45. doi:10.1002/pros.21390

Robert, M., Gibbs, B.F., Jacobson, E., Gagnon, C., 1997. Characterization of prostate-specific antigen proteolytic activity on its major physiological substrate, the sperm motility inhibitor precursor/semenogelin I. Biochemistry 36, 3811–9. doi:10.1021/bi9626158

Salami, S.S., Schmidt, F., Laxman, B., Regan, M.M., Rickman, D.S., Scherr, D., Bueti, G., Siddiqui, J., Tomlins, S.A., Wei, J.T., Chinnaiyan, A.M., Rubin, M.A., Sanda, M.G., 2013. Combining urinary detection of TMPRSS2:ERG and PCA3 with serum PSA to predict diagnosis of prostate cancer. Urol. Oncol. 31, 566–71. doi:10.1016/j.urolonc.2011.04.001

Salimi, A., Kavosi, B., Fathi, F., Hallaj, R., 2013. Highly sensitive immunosensing of prostate-specific antigen based on ionic liquid-carbon nanotubes modified electrode: Application as cancer biomarker for prostate biopsies. Biosens. Bioelectron. 42, 439–446. doi:10.1016/j.bios.2012.10.053

Sanllorente-Méndez, S., Domínguez-Renedo, O., Arcos-Martínez, M.J., 2010. Immobilization of acetylcholinesterase on screen-printed electrodes. Application to the determination of arsenic(III). Sensors (Basel). 10, 2119–28. doi:10.3390/s100302119

Sanllorente-Méndez, S., Domínguez-Renedo, O., Arcos-Martínez, M.J., 2009. Determination of arsenic(III) using platinum nanoparticle-modified screen-printed carbon-based electrodes. Electroanalysis 21, 635–639. doi:10.1002/elan.200804389

Sarkar, A., Hou, H.W., Mahan, A.E., Han, J., Alter, G., 2016. Multiplexed affinity-based separation of proteins and cells using inertial microfluidics. Sci. Rep. 6, 23589. doi:10.1038/srep23589

Sarkar, D., Liu, W., Xie, X., Anselmo, A.C., Mitragotri, S., Banerjee, K., 2014. MoS_2 field-effect transistor for next-generation label-free biosensors. ACS Nano 8, 3992–4003. doi:10.1021/nn5009148

Savory, N., Abe, K., Sode, K., Ikebukuro, K., 2010. Selection of DNA aptamer against prostate specific antigen using a genetic algorithm and application to sensing. Biosens. Bioelectron. 26, 1386–1391. doi:10.1016/j.bios.2010.07.057

Seamonds, B., Yang, N., Anderson, K., Whitaker, B., Shaw, L.M., Bollinger, J.R., 1986. Evaluation of prostate-specific antigen and prostatic acid phosphatase as prostate cancer markers. Urology 28, 472–479. doi:10.1016/0090-4295(86)90146-9

Seo, H.K., Chung, M.K., Ryu, S.B., Lee, K.H., 2007. Detection rate of prostate cancer according to prostate-specific antigen and digital rectal examination in Korean men: A nationwide multicenter study. Urology 70, 1109–12. doi:10.1016/j.urology.2007.07.052

Shafiee, H., Kanakasabapathy, M.K., Juillard, F., Keser, M., Sadasivam, M., Yuksekkaya, M., Hanhauser, E., Henrich, T.J., Kuritzkes, D.R., Kaye, K.M., Demirci, U., 2015. Printed flexible plastic microchip for viral load measurement through quantitative detection of viruses in plasma and saliva. Sci. Rep. 5, 9919. doi:10.1038/srep09919

Siivola, P., Pettersson, K., Piironen, T., Lövgren, T., Lilja, H., Bjartell, A., 2000. Time-resolved fluorescence imaging for specific and quantitative immunodetection of human kallikrein 2 and prostate-specific antigen in prostatic tissue sections. Urology 56, 682–688. doi:10.1016/S0090-4295(00)00671-3

Slawin, K.M., Shariat, S., Canto, E., 2005. BPSA : A novel serum marker for benign prostatic hyperplasia. Rev. Urol. 7, S52–S56.

Small, C.E., Chen, S., Subbiah, J., Amb, C.M., Tsang, S.W., Lai, T.H., Reynolds, J.R., So, F., 2011. High-efficiency inverted dithienogermole–thienopyrrolodione-based polymer solar cells. Nat. Photonics 6, 115–120. doi:10.1038/nphoton.2011.317

Soontornworajit, B., Wang, Y., 2011. Nucleic acid aptamers for clinical diagnosis: Cell detection and molecular imaging. Anal. Bioanal. Chem. 399, 1591–9. doi:10.1007/s00216-010-4559-x

Souada, M., Piro, B., Reisberg, S., Anquetin, G., Noël, V., Pham, M.C., 2015. Label-free electrochemical detection of prostate-specific antigen based on nucleic acid aptamer. Biosens. Bioelectron. 68, 49–54. doi:10.1016/j.bios.2014.12.033

Spain, E., Gilgunn, S., Sharma, S., Adamson, K., Carthy, E., O'Kennedy, R., Forster, R.J., 2016. Detection of prostate-specific antigen based on electrocatalytic platinum nanoparticles conjugated to a recombinant scFv antibody. Biosens. Bioelectron. 77, 759–766. doi:10.1016/j.bios.2015.10.058

Stattin, P., Vickers, A.J., Sjoberg, D.D., Johansson, R., Granfors, T., Johansson, M., Pettersson, K., Scardino, P.T., Hallmans, G., Lilja, H., 2015. Improving the specificity of screening for lethal prostate cancer using prostate-specific antigen and a panel of kallikrein markers: A nested case-control study. Eur. Urol. 68, 207–13. doi:10.1016/j.eururo.2015.01.009

Stern, E., Vacic, A., Rajan, N.K., Criscione, J.M., Park, J., Ilic, B.R., Mooney, D.J., Reed, M.A., Fahmy, T.M., 2010. Label-free biomarker detection from whole blood. Nat. Nanotechnol. 5, 138–142. doi:10.1038/nnano.2009.353

Steuber, T., Niemela, P., Haese, A., Pettersson, K., Erbersdobler, A., Chun, K.H.F., Graefen, M., Kattan, M.W., Huland, H., Lilja, H., 2005. Association of free-prostate specific antigen subfractions and human glandular kallikrein 2 with volume of benign and malignant prostatic tissue. Prostate 63, 13–18. doi:10.1002/pros.20156

Svarovsky, S.A., Joshi, L., 2014. Cancer glycan biomarkers and their detection – past, present and future. Anal. Methods 6, 3918. doi:10.1039/c3ay42243g

Svobodova, M., Bunka, D.H.J., Nadal, P., Stockley, P.G., O'Sullivan, C.K., 2013. Selection of 2′F-modified RNA aptamers against prostate-specific antigen and their evaluation for diagnostic and therapeutic applications. Anal. Bioanal. Chem. 405, 9149–9157. doi:10.1007/s00216-013-7350-y

Tan, C.M., Md Arshad, M.K., Fathil, M.F.M., Adzhri, R., M. Nuzaihan, M.N., Ruslinda, A.R., Ibau, C., Hashim, U., 2016. Interdigitated electrodes integrated with zinc oxide nanoparticles for cardiac troponin I biomarker detection, in: 2016 IEEE International Conference on Semiconductor Electronics (ICSE). IEEE, Kuala Lumpur, pp. 220–223. doi:10.1109/SMELEC.2016.7573631

Tang, Z., Fu, Y., Ma, Z., 2017. Bovine serum albumin as an effective sensitivity enhancer for peptide-based amperometric biosensor for ultrasensitive detection of prostate-specific antigen. Biosens. Bioelectron. 94, 394–399. doi:10.1016/j.bios.2017.03.030

Temiz, Y., Lovchik, R.D., Kaigala, G. V, Delamarche, E., 2015. Lab-on-a-chip devices: How to close and plug the lab? Microelectron. Eng. 132, 156–175. doi:10.1016/j.mee.2014.10.013

Tian, J., Huang, J., Zhao, Y., Zhao, S., 2012. Electrochemical immunosensor for prostate-specific antigen using a glassy carbon electrode modified with a nanocomposite containing gold nanoparticles supported with starch-functionalized multi-walled carbon nanotubes. Microchim. Acta 178, 81–88. doi:10.1007/s00604-012-0816-3

Tombelli, S., Minunni, M., Mascini, M., 2005. Analytical applications of aptamers. Biosens. Bioelectron. 20, 2424–2434. doi:10.1016/j.bios.2004.11.006

Valencia, P.M., Farokhzad, O.C., Karnik, R., Langer, R., 2012. Microfluidic technologies for accelerating the clinical translation of nanoparticles. Nat. Nanotechnol. 7, 623–629. doi:10.1038/nnano.2012.168

Vickers, A.J., Gupta, A., Savage, C.J., Pettersson, K., Dahlin, A., Bjartell, A., Manjer, J., Scardino, P.T., Ulmert, D., Lilja, H., 2011. A panel of kallikrein marker predicts prostate cancer in a large, population-based cohort followed for 15 years without screening. Cancer Epidemiol. Biomarkers Prev. 20, 255–61. doi:10.1158/1055-9965.EPI-10-1003

Walji, N., Chan, A.K., Peake, D.R., 2008. Common acute oncological emergencies: Diagnosis, investigation and management. Postgrad. Med. J. 84, 418–27. doi:10.1136/pgmj.2007.067033

Wang, H., Zhang, Y., Yu, H., Wu, D., Ma, H., Li, H., Du, B., Wei, Q., 2013. Label-free electrochemical immunosensor for prostate-specific antigen based on silver hybridized mesoporous silica nanoparticles. Anal. Biochem. 434, 123–127. doi:10.1016/j.ab.2012.11.012

Wang, J., 2006. Electrochemical biosensors: Towards point-of-care cancer diagnostics. Biosens. Bioelectron. 21, 1887–1892. doi:10.1016/j.bios.2005.10.027

Wang, L., Wang, R., Kong, B.W., Jin, S., Ye, K., Fang, W., Li, Y., 2015. B cells using calcium signaling for specific and rapid detection of Escherichia coli O157:H7. Sci. Rep. 5, 10598. doi:10.1038/srep10598

Wang, L., Wang, Y., Wong, J.I., Palacios, T., Kong, J., Yang, H.Y., 2014. Functionalized MoS_2 nanosheet-based field-effect biosensor for label-free sensitive detection of cancer marker proteins in solution. Small 10, 1101–1105. doi:10.1002/smll.201302081

Wang, M.C., Valenzuela, L.A., Murphy, G.P., Chu, T.M., 1979. Purification of a Human Prostate Specific Antigen. Invest. Urol. 17, 159–163.

Wang, Y., Qu, Y., Liu, G., Hou, X., Huang, Y., Wu, W., Wu, K., Li, C., 2015. Electrochemical immunoassay for the prostate specific antigen using a reduced graphene oxide functionalized with a high molecular-weight silk peptide. Microchim. Acta 182, 2061–2067. doi:10.1007/s00604-015-1552-2

Wilson, D.S., Nock, S., 2002. Functional protein microarrays. Curr. Opin. Chem. Biol. 6, 81–85. doi:10.1016/S1367-5931(01)00281-2

Wu, D., Li, R., Wang, H., Liu, S., Wang, H., Wei, Q., Du, B., 2012. Hollow mesoporous silica microspheres as sensitive labels for immunoassay of prostate-specific antigen. Analyst 137, 608–613. doi:10.1039/c2an16033a

Yan, M., Zang, D., Ge, S., Ge, L., Yu, J., 2012. A disposable electrochemical immunosensor based on carbon screen-printed electrodes for the detection of prostate specific antigen. Biosens. Bioelectron. 38, 355–361. doi:10.1016/j.bios.2012.06.019

Yang, J., Wen, W., Zhang, X., Wang, S., 2015. Electrochemical immunosensor for the prostate-specific antigen detection based on carbon nanotube and gold nanoparticle amplification strategy. Microchim. Acta 182, 1855–1861. doi:10.1007/s00604-015-1523-7

Yang, R., Pagaduan, J. V, Yu, M., Woolley, A.T., 2015. On-chip pre-concentration and fluorescence labeling of model proteins by use of monolithic columns: Device fabrication, optimization, and automation. Anal. Bioanal. Chem. 407, 737–747. doi:10.1007/s00216-014-7988-0

Yang, W.J., Lee, D.H., Chung, B.H., Cho, J.S., Choi, Y.D., Kim, S.J., Cho, I.R., Kim, H.S., Kim, C. Il, Hong, S.J., Members of the Severance Urologic Oncology Group, 2006. Detection rate of prostate cancer on biopsy according to serum prostate-specific antigen in Korean men: A multicenter study. Urology 67, 333–336. doi:10.1016/j.urology.2005.08.027

Yang, Z., Kasprzyk-Hordern, B., Goggins, S., Frost, C.G., Estrela, P., 2015. A novel immobilization strategy for electrochemical detection of cancer biomarkers: DNA-directed immobilization of aptamer sensors for sensitive detection of prostate-specific antigens. Analyst 140, 2628–2633. doi:10.1039/C4AN02277G

Yousuff, C.M., Ho, E.T.W., Hussain K., I., Hamid, N.H., 2017. Microfluidic platform for cell isolation and manipulation based on cell properties. Micromachines 8, 15. doi:10.3390/mi8010015

Zaouak, O., Authier, L., Cugnet, C., Castetbon, A., Potin-Gautier, M., 2010. Electroanalytical device for cadmium speciation in waters. Part 1: Development and characterization of a reliable screen-printed sensor. Electroanalysis 22, 1151–1158. doi:10.1002/elan.200900474

Zapatero-Rodríguez, J., Liébana, S., Sharma, S., Gilgunn, S., Drago, G.A., O'Kennedy, R., 2017. Detection of free prostate-specific antigen using a novel single-chain antibody (scAb)-based magneto-immunosensor. Bionanoscience. doi:10.1007/s12668-017-0394-2

Zen, J.M., Song, Y.S., Chung, H.H., Hsu, C.T., Kumar, A.S., 2002. Photoelectrochemical oxygen sensor using copper-plated screen-printed carbon electrodes. Anal. Chem. 74, 6126–6130. doi:10.1021/ac020058r

Zhan, Y., Liu, Z., Najmaei, S., Ajayan, P.M., Lou, J., 2012. Large-area vapor-phase growth and characterization of MoS_2 atomic layers on a SiO_2 substrate. Small 8, 966–971. doi:10.1002/smll.201102654

Zhang, A., Lieber, C.M., 2016. Nano-bioelectronics. Chem. Rev. 116, 215–257. doi:10.1021/acs.chemrev.5b00608

Zhang, G.J., Ning, Y., 2012. Silicon nanowire biosensor and its applications in disease diagnostics: A review. Anal. Chim. Acta 749, 1–15. doi:10.1016/j.aca.2012.08.035

Zhao, J., Guo, Z., Feng, D., Guo, J., Wang, J., Zhang, Y., 2015. Simultaneous electrochemical immunosensing of alpha-fetoprotein and prostate specific antigen using a glassy carbon electrode modified with gold nanoparticle-coated silica nanospheres and decorated with Azure A or ferrocenecarboxylic acid. Microchim. Acta 182, 2435–2442. doi:10.1007/s00604-015-1591-8

Zhao, Y., Trewyn, B.G., Slowing, I.I., Lin, V.S.Y., 2009. Mesoporous silica nanoparticle-based double drug delivery system for glucose-responsive controlled release of insulin and cyclic AMP. J. Am. Chem. Soc. 131, 8398–8400. doi:10.1021/ja901831u

Zheng, G., Gao, X.P.A., Lieber, C.M., 2010. Frequency domain detection of biomolecules using silicon nanowire biosensors. Nano Lett. 10, 3179–3183. doi:10.1021/nl1020975

Zheng, G., Patolsky, F., Cui, Y., Wang, W.U., Lieber, C.M., 2005. Multiplexed electrical detection of cancer markers with nanowire sensor arrays. Nat. Biotechnol. 23, 1294–1301. doi:10.1038/nbt1138

Zhou, W., Dai, X., Fu, T.M., Xie, C., Liu, J., Lieber, C.M., 2014. Long-term stability of nanowire nanoelectronics in physiological environments. Nano Lett. 14, 1614–1619. doi:10.1021/nl500070h

Zhu, X., Feng, C., Ye, Z., Chen, Y., Li, G., 2014. Fabrication of magneto-controlled moveable architecture to develop reusable electrochemical biosensors. Sci. Rep. 4, 4169. doi:10.1038/srep04169

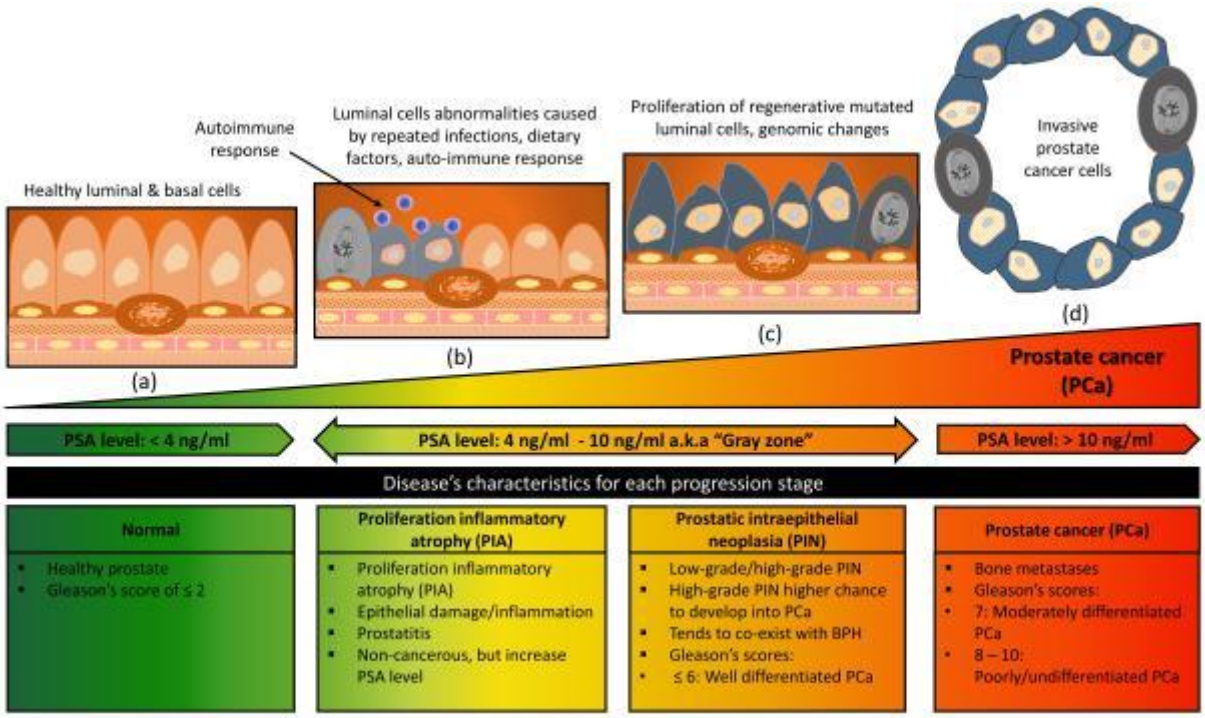

Fig. 1. The epigenetic stages of PCa. (a) shows the transition stage of normal prostate cells into proliferative inflammatory neoplasia (PIA) due to infiltration of lymphocytes, macrophages, or neutrophils. The release of reactive oxygen and nitrogen by phagocytes causing DNA damage, cell injury, and cell death. (b) and (c) show the transition of PIA into prostatic intraepithelial neoplasia (PIN). Two classification of PIN being Low-grade PIN (LGPIN) and High-grade PIN (HGPIN), in which HGPIN is more susceptible for transition into benign prostatic hyperplasia (BPH) and prostate cancer (PCa). This is the diagnostic 'gray zone' that often lead to overtreatment of the disease. (d) depicts the fully transitioned invasive carcinomas of prostatic epithelial cells due to the continued proliferation of genetically unstable luminal cells and accumulation of genomic changes.

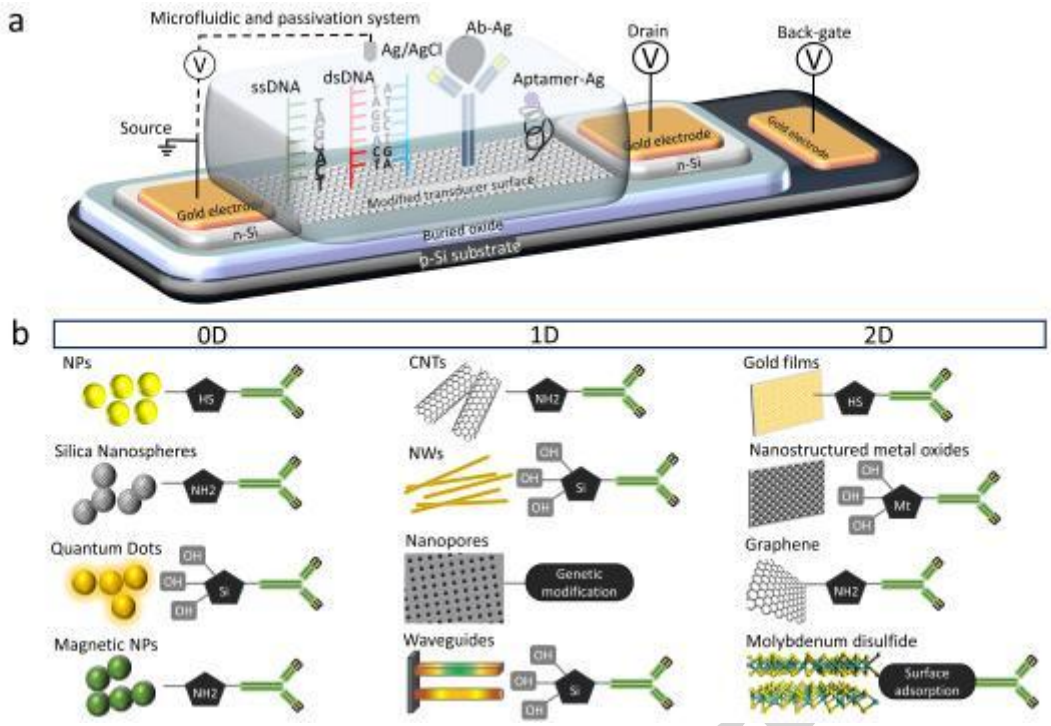

Fig. 2. Typical device structure of FET-based biosensor and the common transducer's modification methodologies. (a) 4-electrodes FET-based biosensors with an integrated fluidic delivery system (i.e. micro-channels), device passivation (i.e. insulating PDMS polymer), and back-gate terminal for ambipolar switching conduction. (b) The transducer's modification techniques and immobilization strategies commonly implemented to amplify the signal transduction of the FET-biosensors in order to achieve high detection sensitivity and lowest LOD. The strategies depicted are grouped into three classifications based on the types of atomic layers i.e. zero-dimensional (0D), one-dimensional (1D), and two-dimensional (2D) materials.

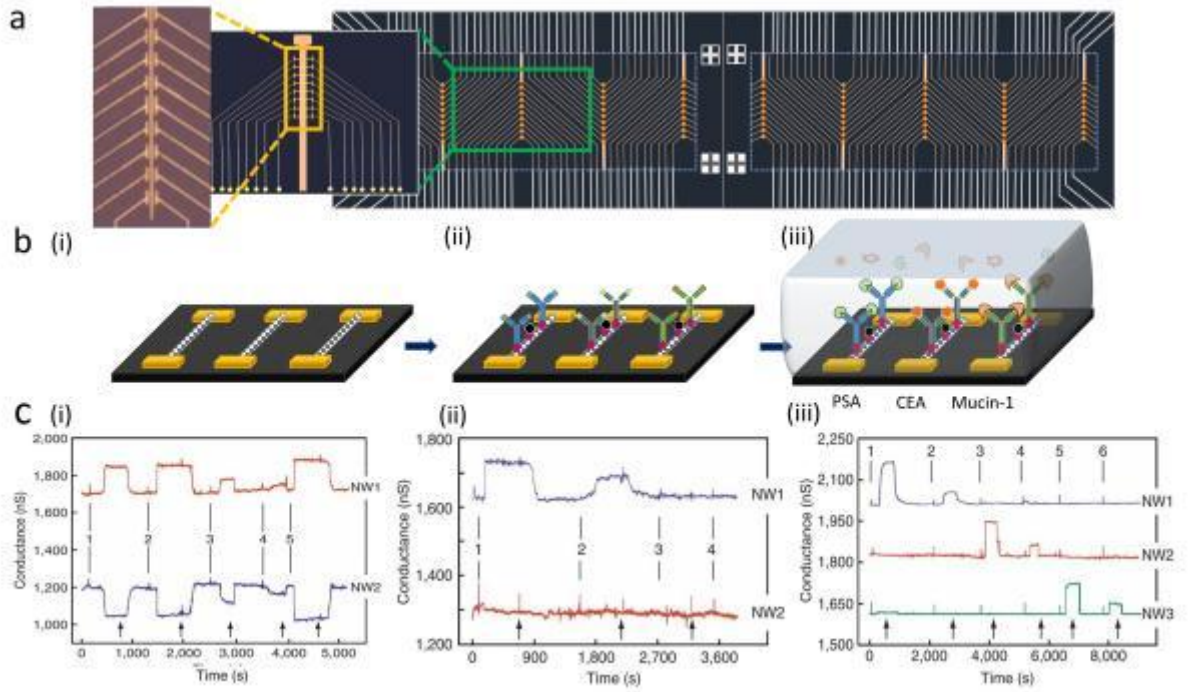

Fig. 3. Multiplexed Si-NWFET immunosensors array, integrated with microfluidic delivery system for label-free, real-time and simultaneous femto-molar ranges detection of PSA, CEA, and mucin-1 antigens. (a) Optical images of NWFET array. The actual NWFET device (left-most) is reprinted with permission from (Zhang and Lieber, 2016). Copyright 2015 American Chemical Society. (b) The assay's surface modification to antigens detection steps. (i) Oxygen-plasma cleaned coupled with APTMS surface treatment to promote aldehyde group on NW surface. (ii) monoclonal antibodies, mAbs immobilization and ethanolamine treatment to block non-specific bindings. (iii) Microfluidic integration for simultaneous detection of antigens. (c) High sensitivity detection of antigens. (i) Conductance change in complementary detection of PSA antigen using the p-type (NW1) and n-type (NW2) Si-NWFET. (ii) Conductance change of p-type NWFET tested on the immobilized PSA mAb1 (NW1) and ethanolamine (NW2), showing successful blocking of non-specific bindings after the application of antigens. (iii) Simultaneous detection of PSA (NW1), CEA (NW2) and mucin-1 (NW3) antigens on p-type Si-NWFET sensors array. Reprinted with permission from (Zheng et al., 2005). Copyright 2005 Nature Publishing Group.

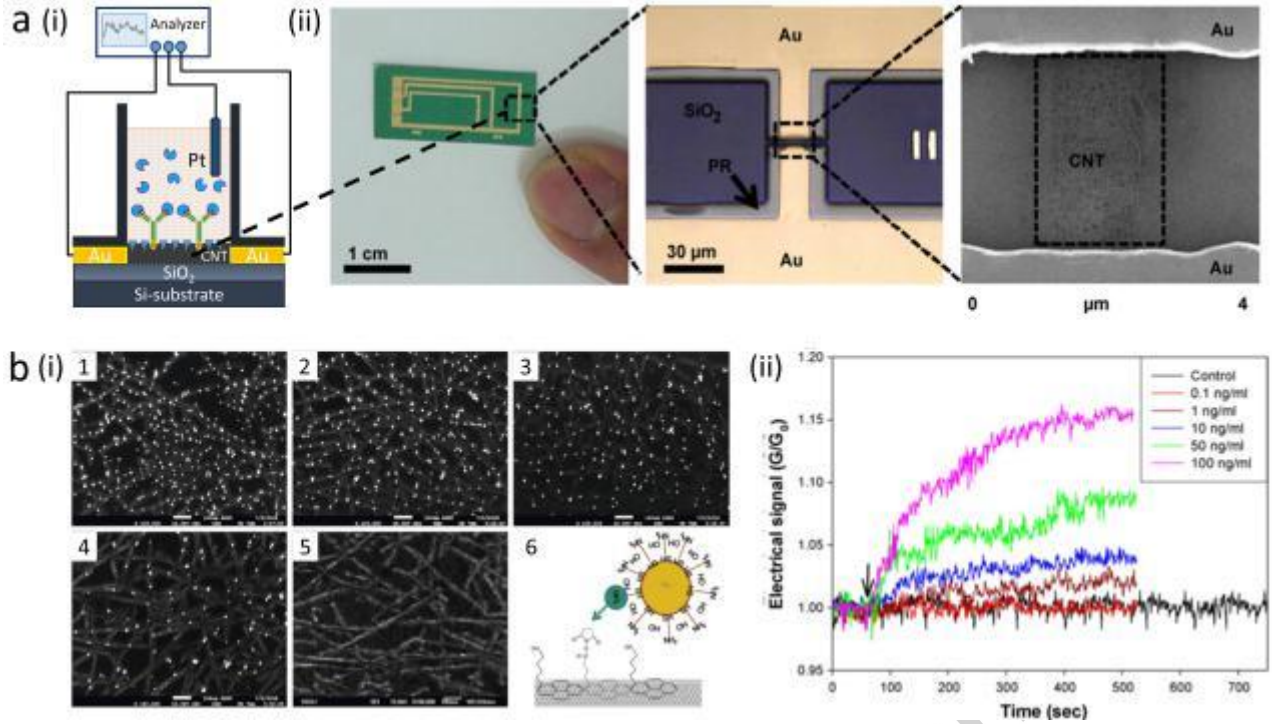

Fig. 4. Optical images of SWCNT-functionalized FET sensor surface using the mixed solution of 1-pyrenebutonoic acid succinimidyl ester (PASE) as linker, and 1-Pyrenbutanol (PB) as spacer at different mixing ratio. (a)(i) The schematic of electrical I-V measurement setup for serum PSA detection and, (a)(ii) optical images of functionalized SWCNT on FET transducer. (b)(i) The SEM images of channel area when 12 nm AuNPs were introduced, (1) AuNPs on PASE only, (2) AuNPs on PASE/PB at 1:1 ratio, (3) AuNPs on PASE/PB at 1:3 ratio, (4) AuNPs on PASE/PB at 1:9 ratio, (5) AuNPs on PB spacer only, and (6) schematic of AuNPs bound to PASE/PB on the CNT-FET functionalized surface. (b)(ii) Electrical I-V response shows high sensitivity detection of PSA under different PSA concentration. Reprinted with permission from (Kim et al., 2009). Copyright 2009 Elsevier B.V.

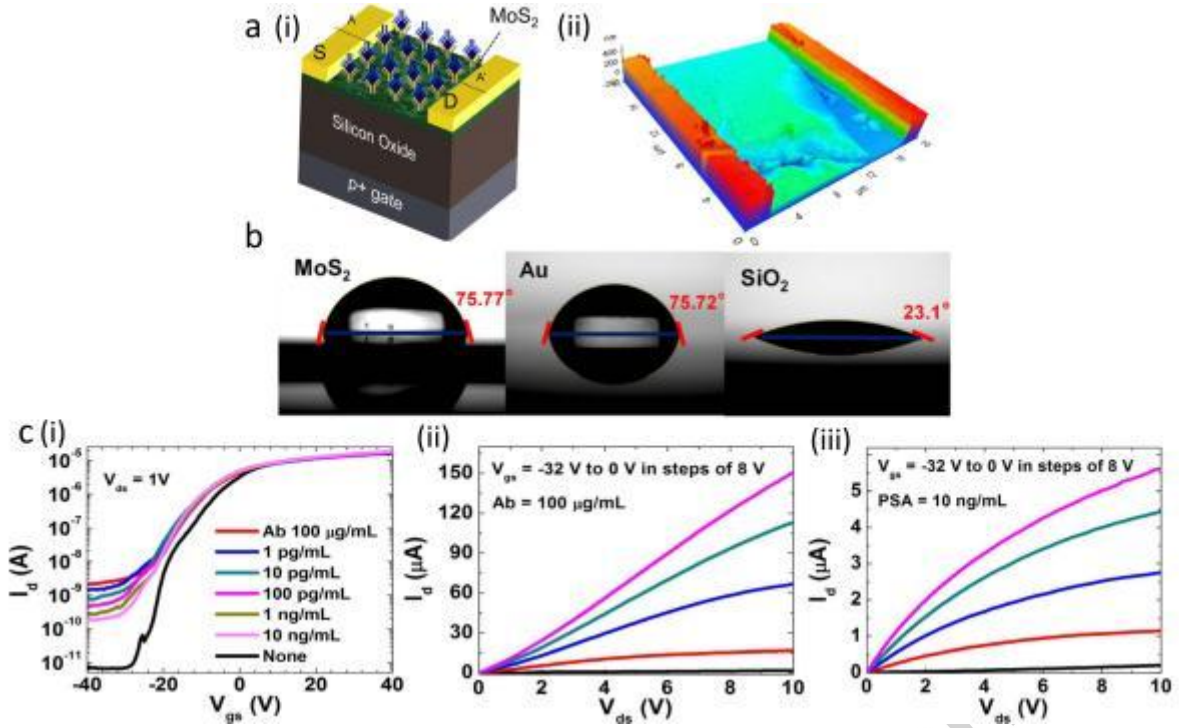

Fig. 5. MoS_2-based FET biosensor. (a)(i) Schematic image of MoS_2 functionalized dielectric-less transducer surface between source-drain terminals, and (a)(ii) Optical image of 3D AFM topography of ~80 nm thick MoS_2 layer. (b) Water contact angle measurement shows high hydrophobicity of MoS_2 compared to Au and SiO_2 substrate, which translates into superiority of MoS_2 for biomolecules functionalization on its surface. (c) Typical electrical I-V measurement for detection of varied concentrations of serum PSA. (c)(i) I-V transfer characteristics of MoS_2-FET for immobilized 100 µg/ml of anti-PSA, and mAb binding to PSA-Ag at concentration ranges 1 pg/ml – 10 ng/ml. (c)(ii) $I_d - V_{ds}$ output response of immobilized 100 µg/ml anti-PSA under back-gate bias effect, V_{gs} of -32 V to 0 V (8 V steps). (c)(iii) ~10-fold reduction in $I_d - V_{ds}$ output response during mAb-Ag binding at fixed PSA concentration of 10 ng/ml, under back-gate bias V_{gs} of -32 V to 0 V (8 V steps). Reprinted with permission from (Lee et al., 2014). Copyright 2014 Nature Publishing Group.

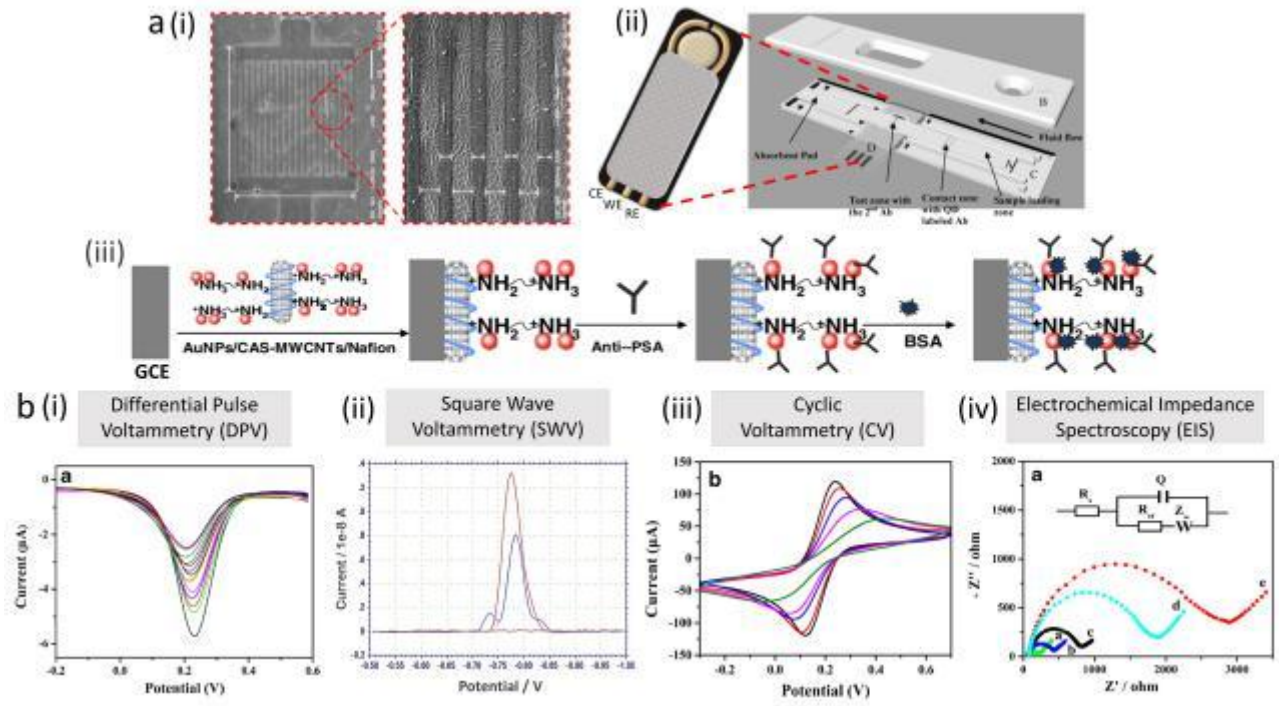

Fig. 6. Images of customized-electrodes devices-based structures, (a)(i) IDE. Reprinted with permission from (Tan et al., 2016). Copyright 2016 IEEE. (a)(ii) Screen-printed electrode (SPE)-integrated immunochromatographic electrochemical biosensor (IEB). Reprinted with permission from (Lin et al., 2008). Copyright 2008 Elsevier B.V. (a)(iii) GCE with functionalized sensing surface. Reprinted with permission from (Tian et al., 2012). Copyright 2012 Springer Vienna. (b) Typical PSA concentration measurement methods. (b)(i) Differential Pulse Voltammetry (DPV), (b)(ii) Square Wave Voltammetry (SWV), (b)(iii) Cyclic Voltammetry (CV), and (b)(iv) Electrochemical Impedance Spectroscopy (EIS). Images b(i), b(iii), and b(iv) are reprinted with permission from (Y. Wang et al., 2015). Copyright 2015 Springer Vienna. Image b(ii) is reprinted with permission from (Lin et al., 2008). Copyright 2008 Elsevier B.V.

Table 1 Conditions of unipolar conductance of the transducer

Transducer doping characteristics	**Biomolecule charges**	**Carrier generation at the transducer**	**Conductivity on the transducer**
n-type (Electron as carrier)	Negative	Fewer electron (More holes)	Decrease
	Positive	More electron (Fewer holes)	Increase
p-type (Holes as carrier)	Negative	More holes (Fewer electron)	Increase
	Positive	Fewer holes (More electron)	Decrease

TABLE 2 Current-based and capacitance-based bioelectronic immunosensors for detection of serum PSA

Detection Method	Antigen	Immobilization strategy	Sample volume	Blocking agent	Lowest detection limit	Assay principle	Ref
Field-Effect Transistors-Based Bioelectronics							
n-type Poly-SiNWs-FET	PSA	Poly-SiNWs/APTES/GA/anti-PSA/ PSA	Flow in microfluidic channel at rate of 83 ul/min	Tween 20	500 pg/mL to 5 fg/mL	I-V measurement	(Huang et al., 2013)
Multiplexed SiNWs-FET	fPSA/ PSA-ACT complex/CEA/mucin-1	SiNWs/APTMS/anti-MAb (anti-fPSA/ anti-ACT-PSA/anti-CEA/anti-mucin-1) /Antigen (fPSA/PSA-ACT/CEA/mucin-1)	Flow in microfluidic channel at rate of 0.15 ml/h	Ethanolamine	LOD: 5 fg/ml PSA: 75 fg/ml CEA: 100 fg/ml Mucin-1: 75 fg/ml	Conductance	(Zheng et al., 2005)
AuNPs-anti-PSA half fragment conjugates on SiNWs-FET	PSA	SiNWs/GOPS-SH/AuNPs-anti-PSA half fragment conjugates/PSA	100 µl	Tween 20/BSA	At SNR>3 500 ng/ml – 23 fg/ml LOD: 23 fg/ml CV: 0.97	I-V measurement	(Presnova et al., 2017)
SWCNT-FET	PSA-ACT	SiO2/methyl-terminated OTS SAM/SWCNTs/PASE(linker)/PB(spacer)/PSA-ACT MAb/ PSA-ACT	5.0 ul	Ethanolamine	1.0 ng/ml	I-V measurement	(Kim et al., 2009)
SWCNTs/Metal oxide Si-NWs hybrid	PSA	NWs/SWCNTs: Si/SiO_2/PASE/PSA MAb/PSA NWs: Si/SiO_2/In2O3/carboxylate succinimidyl ester/PSA Ab/PSA	N/A	BSA	5 ng/ml	I-V measurement	(Li et al., 2005)
Pt-microelectrodes-modified SWCNTs	tPSA	SiO_2/Pt/SWNTs/PASE/anti-tPSA MAb/tPSA	N/A	BSA/ ethanolamine	0.25 ng/ml	DPV	(Okuno et al., 2007)
SWCNTs forest immuno	PSA/PSMA/PF-4/IL-6	SiO2/Pt/SWNTs/EDC/NHS/anti-Ab_1(anti-PSA, anti-PSMA, anti-PF-4, anti-IL-	10 µl	Casein/ Twee	PSA: 1 ng/ml PSMA:	Amperometric	(Chikkaveeraia

array		6)/Ag (PSA, PSMA, PF-4, IL-6)/Ab_2-conjugate* *PSA/PSMA: Ab_2(anti-PSA/anti-PSMA)-HRP conjugated *PF-4/IL-6: biotinylated-Ab_2(anti-PF-4/anti-IL-6)-streptavidin-HRP conjugated H_2O_2 redox, hydroquinone mediator		n 20	10 ng/ml PF-4: 1 ng/ml IL-6: 0.03 ng/ml		h et al., 2009)
MoS_2 on FET	PSA	MoS_2/HfO_2/APTES/GA/anti-PSA MAb/PSA	N/A	BSA	Sensitivity: down to 375 fM	I-V measurement	(Wang et al., 2014)
SiO_2-MoS_2 on FET	PSA	Si/SiO_2/MoS_2/anti-PSA MAb/PSA	N/A	N/A	LOD: 1 pg/ml	I-V measurement	(Lee et al., 2014)
Customized-Electrodes Devices-Based Bioelectronics							
IL-based MWCNTs nanocomposite	PSA	GCE/IL-MWCNTs/anti-PSA MAb_1/PSA/anti-PSA MAb_2 labeled HRP *Thionine as redox	N/A	BSA	20 pg/ml at SNR > 3	CV	(Salimi et al., 2013)
AuNPs-MWCNTs on GCE	tPSA	GCE/MWCNTs/EDC/NHS/anti-tPSA Ab_1/tPSA/anti-tPSA Ab_2/Fc/AuNPs Incubation: 75 min at 37°C 5 mM $K_3[Fe(CN)_6]/K_4[Fe(CN)_6]$ redox probe solution	10 µl	BSA	5.4 pg/ml Range: 0.01-100 ng/ml	CV/EIS	(Yang et al., 2015)
AuNPs-MWCNTs on GCE	PSA	GCE/CAS-MWCNTs/AuNPs/Anti-PSA MAb/PSA	1 ml	BSA	7 pg/ml at SNR =3	CV/EIS (Impedimetric)	(Tian et al., 2012)
Ag@MSN-modified on GCE	PSA	GCE/Ag@MSN/GA/anti-PSA/PSA *hydroquinone as mediator/redox	5 µl	BSA	0.05 ng/ml – 50 ng/ml LOD: 15 pg/ml at SNR = 3	CV	(Wang et al., 2013)
AuNPs/rGO modified on GCE	AFP/PSA	GCE/rGO-AuNPs/anti-Ab1 (anti-AFP and anti-PSA)/PSA/secondary Ab_2-bioconjugates labels**	20 µl	BSA	AFP: 0.01 ng/ml – 25 ng/ml LOD:	DPV	(Zhao et al., 2015)

		**AFP: anti-AFP@Azure A-Ab_2-Si@AuNPs conjugate **PSA: anti-PSA@Fc-Ab_2-Si@AuNPs conjugate #Redox – Azure A and Fc			3.3 pg/ml (SNR= 3 PSA: 0.012 ng/ml – 25 ng/ml LOD: 4.0 pg/ml (SNR= 3)		
SP-rGO modified on GCE	PSA	GCE/SP-rGO-GA/anti-PSA MAb/PSA *redox: hexacyanoferrate *incubate: 30 min	N/A	BSA	0.1 ng/ml – 5.0 ng/ml 5.0 ng/ml – 80.0 ng/ml LOD: 53 pg/ml (SNR= 3)	CV/EIS	(Wang et al., 2015)
HSMs modified on GCE	PSA	GCE/NPG/anti-PSA MAb_1/PSA/anti-PSA MAb_2-HRP-TH-HSMs nanoparticles	N/A	BSA	0.01 ng/ml – 10 ng/ml LOD: 6.0 pg/ml	CV/EIS (Amperometric)	(Wu et al., 2012)
PAMAM-AuNPs-enzyme linked aptamer modified on GCE	PSA	GCE/rGO-chitosan/GA/TH†-anti-PSA MAb_1-TH/PSA/aptamer* conjugate** *Aptamer sequence: Aptamer: (5'-NH2-(CH2)6-ATTAAAGCTCGCCATCAAA TAGC-3') and Aptamer-biotin: (5'-NH2-(CH2)6-ATTAAAGCTCGCCATCAAATAGC-biotin3') **AuNPs-PAMA/NH_2-aptamer, and AuNPs-PAMA/ NH_2-aptamer-biotin/strep-HRP †redox agent	10 µl	BSA	0.1 pg/ml – 90 ng/ml LOD: 10 fg/ml	DPV/EIS	(Kavosi et al., 2015)
PS-Fc	PSA	GCE/GO-	N/A	BSA	0.01	Strippi	(Ding

modified on GCE		(EDC/NHS)/anti-PSA MAb_1/PSA/ anti-PSA MAb_2-(chitosan)-PS-Fc Incubate: 1 hour at RT			ng/ml – 20 ng/ml LOD: 1 pg/ml	ng voltammetry (CV/EIS/SWV)	et al., 2013)
IEB-LOC on glass-fiber SPE	PSA	Glass/nitrocellulose membrane/GA/anti-PSA/PSA/anti-PSA-QD conjugated	100 ul	BSA	0.05 ng/ml – 4 ng/ml LOD: 0.02 ng/ml	SWV	(Lin et al., 2008)
DTSP-SAM IDE	PSA	Cr-Au/DTSP-SAM/anti-PSA MAb/PSA	N/A	Ethanolamine	100 pg/ml – 1 pg/ml	Impedimetric	(Chornokur et al., 2011)
Cys-SAM IDE	PSA	Cr-Au/Cys-SAM/EDC-NHS/anti-PSA MAb/PSA	N/A	BSA	100 ng/ml - 1 pg/ml	Impedimetric	(Arya and Bhansali, 2012)
Micro-gapped interdigitated (MGIDEA)	PSA	Ti-Au bilayer/APTES/GA/anti-PSA140 MAb/PSA/anti-PSA103-ALP conjugated/Ag deposit	20 µl	BSA	0.9 pg/l Linear: 1.0 pg/l to 1.0 µg/l	LSV (conductance)	(Huang et al., 2009)
SPE	fPSA/tPSA	Au/anti-PSA/PSA/biotin-streptavidin-AP label/Ag deposit	40 µl	Casein	10 ng/ml – 100 ng/ml 1 ng/ml – 10 ng/ml	LSV	(Escamilla-Gomez et al., 2009)
PANI modified -carbon SPE	PSA	1. Poly(1,2-DAB)-PANI-anti-PSA entrapment/PSA 2. Poly(1,2-DAB)-PANI/avidin-biotin/biotinylated anti-PSA/PSA *Redox mediator: 10 mmol/L, 50:50 mixed ratio of $Fe(CN)_6^{3-/4-}$	N/A	BSA, HSA, CA125, NSE, S-100[β]	1. 1 to 200 ng/ml. LOD: 1 ng/ml 2. 1 pg/ml to 100 pg/ml.	Impedimetric	(Barton et al., 2008)

NH_2-*Functionalized Graphene on SPE*	PSA	GR-NH_2/GA/anti-PSA/PSA/HRP-anti-PSA conjugated/colloidal AuNPs	10 µl	BSA	LOD: 1 pg/ml 0.002 ng/ml – 2.0 µg/ml LOD: 0.46 pg/ml (SNR =3)	LSV/CV (Impedimetric)	(Yan et al., 2012)
Magneto-based, MPs-scAb conjugated on carbon SPE	fPSA	Carbon-GCE/MPs-anti-fPSA scAb conjugates/fPSA/HRP-anti fPSA Ab_2 conjugates *Mediator: H_2O_2/hydroquinone	N/A	BSA	0 ng/ml – 10 ng/ml LOD: 0.5 ng/ml DR: 10 ng/ml (R^2=0.9979) CV: 8-12%	Amperometric/CV	(Zapatero-Rodríguez et al., 2017)
PtNPs-scFv Ab conjugates on Au disc electrode	PSA/fPSA	Au/L-cysteine-SAM/EDC-NHS/anti-PSA mAb/PSA/PtNPs-anti-PSA scFv B8 conjugates	N/A	BSA	1 ng/ml – 30 ng/ml LOD: 0.03 ng/ml	Amperometric (CV/EIS)	(Spain et al., 2016)
Peptide cleavage on GCE	PSA	GCE/GO-PDDA-$Pb_2[Fe(CN)_6]$-chitosan/peptide-IL/BSA/PSA * Redox: $Pb_2[Fe(CN)_6]$	80 µl	BSA	100 ng/ml – 1 fg/ml LOD: 1 fg/ml	Amperometric (EIS)	(Tang et al., 2017)

Highlights

- A concise review on immunosensor for prostate cancer's detection is presented.
- The field-effect transistors and customized-electrodes devices-based sensors offer the highest LODs and portability.
- The future visions of prostate-specific antigen (PSA) biosensing are discussed.